CJMR

Current Journal of Medical Research

Vol: 5 Issue: 1 Year: 2025

ISSN: 2791-7061

ABOUT CJMR

Current Journal of Medical Research in Health Sciences is an international, refereed, scientific journal published three times a year (April, August and December) in English. CJMR is a free, open access journal.

İZMİR KÂTİP ÇELEBİ UNIVERSITY
2010

CJMR
Current Journal of Medical Research
Vol:5 **Issue:**1 **30 Nisan 2025**

Publisher/Yayıncı
Izmir Katip Celebi University Faculty of Medicine
(İzmir Kâtip Çelebi Üniversitesi Tıp Fakültesi)

Privilege Owner
Prof. Dr. Saffet KOSE (Rector)
Izmir Katip Celebi University

ISSN
2791-7061

Journal Type: Peer Review Journal

Language: English

Publication Period: Quarterly

PUBLICATION OR ADVISORY BOARD

BASIC MEDICAL SCIENCES

INTERNAL MEDICAL SCIENCES

SURGICAL MEDICAL SCIENCES

İÇİNDEKİLER

CONTENTS

DETERMINING SERUM ASYMMETRIC DIMETHYLARGININE (ADMA) LEVEL IN COVID-19 PNEUMONIA AND ITS RELATION WITH THROMBOSIS AND MORTALITY ADMA LEVEL IN COVID-19 PNEUMONIA

COVİD-19 PNÖMONİSİNDE SERUM ASİMETRİK DİMETİLARJİNİN (ADMA) DÜZEYİNİN TESPİTİ VE TROMBOZ, MORTALİTE İLE İLİŞKİSİNİN BELİRLENMESİ COVİD-19 PNÖMONİSİNDE ADMA DÜZEYİNİN TESPİTİ

Tugba CETINTEPE*[1], Ugur Bayram KORKMAZ[2], Leyla DEMIR[3], Salih Atakan NEMLI[4], Tugba Oncel VAN[5], Lutfi CETINTEPE[6], Serife SOLMAZ[7], Ahmet ALACACIOGLU[8]

[1]Department of Hematology, Izmir Katip Celebi University, Ataturk Training and Research Hospital, Izmir, Türkiye. e-mail: tugbacetintepe@gmail.com
[2]Department of Internal Medicine, Izmir Katip Celebi University Ataturk Training and Research Hospital, Izmir, Türkiye. e-mail: ugurbk07@gmail.com
[3]Department of Biochemistry, Izmir Katip Celebi University Ataturk Training and Research Hospital, Izmir, Türkiye. e-mail: argunleyla@gmail.com
[4]Department of Infectious Diseases and Clinical Microbiology, Izmir Katip Celebi University Ataturk Training and Research Hospital, Izmir, Türkiye. e-mail: atanemli@yahoo.com
[5]Department of Biochemistry, Izmir Katip Celebi University Ataturk Training and Research Hospital, Izmir, Türkiye. e-mail: tubaoncel@hotmail.com
[6]Department of Nephrology, Izmir Katip Celebi University Ataturk Training and Research Hospital, Izmir, Türkiye. e-mail: lutficetintepe@gmail.com
[7]Department of Hematology, Izmir Katip Celebi University, Ataturk Training and Research Hospital, Izmir, Türkiye. e-mail: solmazserife@yahoo.com
[8]Department of Oncology, Izmir Katip Celebi University, Ataturk Training and Research Hospital, Izmir, Türkiye. e-mail: dralacacioglu@hotmail.com

ORCID ID: TC: 0000-0001-5398-235X **UBK:** 0000-0001-7115-2130 **LD:** 0000-0001-9174-8935 **SAN:** 0000-0002-2720-9870
TOV: 0000-0002-3167-0432 **LC:** 0000-0002-1122-6094 **SS:** 0000-0001-7180-3423 **AA:** 0000-0003-3428-5932

DOI: 10.52818/cjmr.1569445 **E-ISSN:** 2791-7061

ARTICLE INFO

Article Information

Article Type:
Research Article
Received: 17.10.2024
Accepted: 06.04.2025
Published: 30.04.2025

Keywords:
Covid-19 pneumonia, Asymmetric dimethylarginine, ADMA, SOFA, qSOFA, Neutrophil/Lymphocyte ratio, CRP/albümin ratio

ABSTRACT

Objective: COVID-19 can cause widespread inflammation in endothelial cells. Asymmetric dimethylarginine (ADMA) is a molecule recognized as an important marker of vascular endothelial dysfunction. The aim of this study was to determine serum ADMA levels during the course of COVID-19 pneumonia and to assess the relationship between serum ADMA levels, susceptibility to thrombosis, and mortality. Another aim of this study was to identify mortality-associated risk factors and evaluate the effectiveness of different sepsis scores, laboratory measurements, and prognostic markers.

Materials and Methods: Data from 60 patients diagnosed with COVID-19 pneumonia were analyzed. Blood samples for ADMA measurement were collected in the morning within the first three days after symptom onset. Additionally, samples were collected from 60 healthy volunteers to serve as a control group.

Results: The mean serum ADMA level in inpatients with COVID-19 pneumonia was 95.35 ± 223.8 ng/mL, while the mean level in the control group was 266.56 ± 606.14 ng/mL. The ADMA level in COVID-19 patients was found to be significantly lower compared to the control group (p = 0.042). The inpatient mortality rate was 21%. Mortality was significantly associated with higher SOFA and qSOFA scores at admission.

Conclusion: Serum ADMA concentrations measured in the early period of hospitalization were found to be significantly lower in patients with COVID-19 pneumonia compared to the control group. It is important to note that patients with a SOFA score ≥ 3, qSOFA score ≥ 1, CRP/Albumin ratio ≥ 30, and Neutrophil/Lymphocyte Ratio ≥ 5 are at high risk of mortality and require early intervention.

MAKALE BİLGİLERİ

Makale Bilgisi

Makale Türü:
Araştırma Makalesi
Geliş Tarihi: 17.10.2024
Kabul Tarihi: 06.04.2025
Yayım Tarihi : 30.04.2025

Anahtar Kelimeler:
Covid-19 pnömonisi, Asimetrik dimetilarjinin, ADMA, SOFA, qSOFA, Nötrofil/Lenfosit oranı, CRP/albümin oranı

ÖZET

Amaç: Covid-19, endotel hücrelerinde yaygın inflamasyona neden olabilir. Asimetrik dimetilarjinin (ADMA), vasküler endotel disfonksiyonunun önemli belirteçlerinden olarak kabul edilen bir moleküldür. Bu çalışmanın amacı, Covid pnömonisinin seyri sırasında serum ADMA düzeyini saptayıp, serum ADMA düzeyi ile tromboza yatkınlık ve mortalite arasındaki ilişkiyi belirlemektir. Çalışmanın diğer bir amacı da mortaliteyle ilişkili risk faktörlerini belirlemek ve farklı sepsis skorlarının, laboratuvar ölçümlerinin ve prognostik belirteçlerin etkinliğini araştırmaktır.

Gereç ve Yöntemler: Covid-19 pnömonisi tanısı alan 60 hastanın verileri analiz edildi. ADMA için kan örnekleri, pnömonisi olan hastalarda semptom başlangıcından sonraki ilk 3 gün sabah saatlerinde ve 60 sağlıklı gönüllüden alındı.

Bulgular: Hastaneye yatan covid pnömonili hastaların ortalama serum ADMA düzeyi 95,35±223,8 ng/mL idi. Kontrol grubunda ölçülen ortalama serum ADMA düzeyi 266,56±606,14 ng/mL idi. Covid hastalarında ölçülen ADMA değerinin kontrol grubuna göre anlamlı derecede düşük olduğu görüldü. (p 0,042) Yatan hastalardaki ölüm oranı %21 idi. Ölüm oranı, başvuru anında daha yüksek düzeyde saptanan SOFA ve qSOFA düzeyleri ile ilişkiliydi.

Sonuç: Hastaneye yatışın erken döneminde ölçülen serum ADMA konsantrasyonunun Covid-19 pnömonisi olan hastalarda kontrol grubuna göre anlamlı derecede düşük olduğu belirlendi. SOFA skoru≥3, qSOFA skoru≥1, CRP/Albümin oranı≥30 ve Nötrofil/Lenfosit Oranı ≥5 olan vakaların mortalite riskinin yüksek olduğu ve erken müdahale gerektirdiği unutulmamalıdır.

Cetintepe T., Korkmaz UB., Demir L., et al. Determining Serum Asymmetric Dimethylarginine (Adma) Level in Covid-19 Pneumonia and Its Relation With Thrombosis and Mortality. CJMR 2025 5(1):1-11

Correspondence to: Tugba Cetintepe, Department of Hematology, Izmir Katip Celebi University, Ataturk Training and Research Hospital, Izmir, TUrkey
e-mail: tugbacetintepe@gmail.com

Authorship Contributions: T.C.and A.A contributed to the concept, design and to the writing of the manuscript. U.B.K and S.A.N. contributed to data collection. L.D and T.Ö.V helped in the study of biochemical parametres. L.C. S.S, reviewed and provided feedback in the manuscript designing and writing.
Conflict of Interest: The authors declare no conflict of interest
Financial Support: None
Ethics Approval: Approval for the study was granted by Izmir Kâtip Celebi University Clinical Research Ethics Committee (Decision Number: 20221/48)

Introduction

A novel coronavirus causing severe acute respiratory syndrome was identified in 2019 and named COVID-19. The disease, which led to a global pandemic, often progresses with many asymptomatic cases (1). Dyspnea and hypoxemia are indicators of severe disease and typically appear approximately one week after symptom onset (2). Complications in affected patients may include atypical pneumonia, respiratory failure, acute respiratory distress syndrome (ARDS), acute renal failure, venous thromboembolism, pulmonary embolism, disseminated intravascular coagulation (DIC), and death (3).

The upper and lower respiratory tracts are the primary sites of infection in COVID-19 pneumonia. A study by Varga et al. in 2020 provided evidence that COVID-19 can cause widespread inflammation in endothelial cells (4). Exacerbation of endothelial dysfunction may impair organ perfusion and contribute to severe disease progression. In addition to endothelial dysfunction, several other mechanisms—such as disseminated intravascular coagulation syndrome, cytokine storm, antiphospholipid antibody syndrome, macrophage activation syndrome, complement activation, and dysregulation of the renin-angiotensin-aldosterone system—may play a role in the pathogenesis of thrombosis during the course of viral infection.

Asymmetric dimethylarginine (ADMA) is a molecule recognized as an important marker of vascular endothelial dysfunction (5). Nitric oxide (NO), the most important vasodilator produced by the endothelium, plays a key role in maintaining vascular health. ADMA is an endogenous competitive inhibitor of endothelial nitric oxide synthase (eNOS), reducing both the production and bioavailability of NO. A decrease in NO production can contribute to the development and progression of atherosclerosis and thrombosis.

Numerous studies in the literature focus on cytokines, particularly interleukin-6 (IL-6), a key marker of the cytokine storm involved in the pathogenesis of COVID-19 (6). However, the relationship between ADMA—an established marker of endotheliitis—and COVID-19 infection remains unclear.

COVID-19 pneumonia can become life-threatening when complications arise, making it vitally important to identify high-risk patients early and initiate appropriate treatment promptly. Determining which patients require intensive care can be challenging and should be based on individual, patient-centered assessments. However, understanding the key prognostic factors in this clinically complex group can greatly aid in patient management. Therefore, reliable prognostic indicators are essential for identifying severe disease and guiding clinical decisions.

The Quick Sequential Organ Failure Assessment (qSOFA) is a scoring system designed to quickly and easily assess the risk of mortality associated with sepsis, without the need for laboratory tests. It is particularly useful at the time of emergency department presentation (7). In contrast, the Sequential Organ Failure Assessment (SOFA) score is a comprehensive tool developed to predict survival in intensive care patients with severe organ dysfunction or failure. Although it is not intended to diagnose sepsis, it is highly effective in identifying patients at high risk of death (8).

The aim of this study was to determine serum ADMA levels—known to be associated with endothelial dysfunction—during the course of COVID-19 pneumonia, and to assess the relationship between serum ADMA levels,

susceptibility to thrombosis, and mortality. Another objective was to identify mortality-associated risk factors in patients hospitalized with COVID-19 pneumonia and to evaluate the effectiveness of various sepsis scores, laboratory parameters, and prognostic markers in predicting mortality in this clinical population.

Material and Methods

Data from 60 patients admitted to the internal medicine and infectious diseases clinics with a diagnosis of COVID-19 pneumonia were analyzed. Real-time polymerase chain reaction (RT-PCR), the gold standard for diagnosing SARS-CoV-2, was performed on nasal and throat swab samples taken in the emergency department. Regardless of RT-PCR results, patients showing typical signs of COVID-19 pneumonia on thoracic computed tomography (CT) were included in the study.

All patients were isolated and treated according to their individual clinical needs. Depending on disease severity and the presence of respiratory distress, some patients were transferred to the intensive care unit for follow-up. Blood samples for ADMA measurement were collected in the morning within the first three days after symptom onset and stored at –80 °C until analysis. The healthy volunteer group consisted of individuals aged 18–90 years who presented to the internal medicine outpatient clinic, had no history of COVID-19 infection, and no known history of thrombosis. Their blood samples were also collected in the morning.

qSOFA and SOFA scores were calculated for each patient at the time of admission to the clinic, and again upon transfer to the intensive care unit, if applicable. Based on laboratory data obtained at hospital admission, the Neutrophil/Lymphocyte Ratio (NLR), Platelet/Lymphocyte Ratio (PLR), and Monocyte/Lymphocyte Ratio (MLR) were also calculated.

Statistical analysis

Statistical analyses were performed using IBM SPSS Statistics for Windows, Version 25.0 (IBM Corp., Armonk, NY, USA). Descriptive statistics were presented as frequencies and percentages (n, %) for categorical variables, and as mean ± standard deviation (SD) or median with interquartile range (IQR) for continuous variables.

When the data of the study were analyzed in terms of normality assumptions, Independent t-test, one of the parametric tests, was applied to determine whether there was a significant difference between Kolmogorov-Smirnov values between ADMA groups. Cox regression model was used for multivariate analysis. Chi Square test was used to compare categorical variables. receiver operating characteristic (ROC) analysis results regarding the prediction of death by ADMA scores are given. Kaplan-Meier method was used to compare survival times between covid-19 pneumonia and control groups. $p<0.05$ was considered statistically significant. We determined the optimum cutoff points for the SOFA, qSOFA, CAR, NLR, PLR, MLR as a predictor for hospital survival based on the ROC curve. Gender, age, SOFA, qSOFA, CAR, NLR, PLR, MLR scores all were tested in the multivariate analysis. $p < 0.05$ was considered statistically significant.

Measurement of ADMA

Serum ADMA levels in both patient and control groups were analyzed using the enzyme-linked immunosorbent assay (ELISA) method on a Biotek semi-automatic ELISA device (Elabscience, 14780 Memorial Drive, Suite 216, Houston, Texas 77079), employing ELISA kits with a coefficient of variation (CV%) of 10%. After serum samples were thawed at room temperature, precipitated protein molecules at

the bottom were resuspended using a vortex mixer to ensure a homogeneous mixture. The analysis was conducted in accordance with the test procedure provided in the ELISA kit. Serum samples were evaluated using the competitive ELISA method, and absorbance values were measured spectrophotometrically at 450 nm. ADMA concentrations were calculated based on the standard absorbance curve generated from the known standards.

Results

Sixty patients diagnosed with COVID-19 pneumonia and admitted to the clinic were included in this study. Among them, 52 patients (87%) had a positive COVID-19 PCR test, and all cases were confirmed by high-resolution thoracic computed tomography (CT). Sixteen patients experienced a deterioration in their general condition and were transferred to the intensive care unit (ICU). Of these ICU patients, 15 developed respiratory failure. Invasive mechanical ventilation was initiated in 6 patients, noninvasive ventilation in 4, and high-flow oxygen therapy via face mask in 6. One patient was transferred to the ICU due to intracranial hemorrhage. All patients who required invasive mechanical ventilation died. Additionally, 3 patients received positive inotropic or vasopressor support upon ICU admission. In total, 13 of the 16 ICU-admitted patients died.

The characteristics of patients diagnosed with COVID-19 pneumonia and those in the control group are summarized in **Table 1**.

Table 1. *Patients characteristics of Covid-19 pneumonia and control group*

	Control group (n:60)	Covid-19 pneumonia (n:60)	*p*-value
Age (years)	62.86±14	62.5±17	0.90[a]
Gender (male/female)	29/31	24/36	0.36[b]
Hemoglobin (mean±SD.g/dL)	13.38±1.6	11.96±2	**0.0001[a]**
Lymphocyte(mean±SD.10^9/L)	2.6±8.6	1.4±1.5	**0.004[a]**
Platelet (mean±SD.10^9/L)	234±81	226±102	0.63[a]
Albumine (mean±SD. g/L)	4.45±0.3	3.35±0.5	**0.0001[a]**
C-reactive protein (mg/L)	5.89±14	98±84	**0.0001[a]**
eGFR (ml/min)	78±21	69±32	0.07[a]
D-dimer (ng/ml)	164±171	877±140	**0.001[a]**
Ferritin (ug/L)	54.8±59	451±494	**0.0001[a]**
ADMA (ng/ml)	266±56	95.35±223	0.042[a]
LDH (U/L)	167±40	316±166	**0.0001[a]**

[a]:independent t test, [b]:Chi Square test. **GFR,** glomerular filtration rate **ADMA**, asymmetric dimethylarginine **LDH**, Lactic dehydrogenase

The mean serum ADMA level in inpatients with COVID-19 pneumonia was 95.35 ± 223.8 ng/mL (range: 12.2–1705), whereas the mean level in the control group was 266 ng/mL. The ADMA level in COVID-19 patients was significantly lower compared to the control group (p = 0.042).

Receiver Operating Characteristic (ROC) curve analysis was performed to determine the optimal cutoff point for serum ADMA levels. The median ADMA level was 40.88 ng/mL. Based on this cutoff, patients were categorized into two groups: a high ADMA group (≥ 40.88 ng/mL) and a low ADMA group (< 40.88 ng/mL), with a sensitivity of 62% and specificity of 38%. A total of 25 patients (41.6%) had low ADMA levels, while 35 patients (58.3%) had high ADMA levels. According to these classifications, there was no statistically significant association between ADMA levels and survival in the intensive care unit (p = 0.55).

Among the 60 patients included in the study, one developed acute ischemic cerebrovascular disease during hospitalization, and another developed lower extremity arterial thrombosis. Additionally, one patient was treated for a left iliac arterial thrombus one month after discharge. Due to the low number of patients with acute thrombotic events, no statistically significant relationship could be established between thrombosis and serum ADMA levels.

Receiver Operating Characteristic (ROC) curve analysis was performed to determine the optimal cutoff points for the SOFA and qSOFA scores, as well as the NLR, PLR, MLR, and CAR ratios (**Table 2**). Patients with high SOFA scores were found to have significantly longer hospital stays (p = 0.0001).

Table 2. *Roc curve analysis for Covid-19 pneumonia patients.*

	Cut-off	Sensitivity %	Spesificity %	p
SOFA	2,5	62	38	0,0001*
qSOFA	0,5	20	77	0.008*
NLR	5,52	53	45	0,003*
PLR	189,83	46	53	0,34
LMR	0,40	54	40	0,12
CAR	29,36	31	69	0,05*
AST/ALT	1,33	40	54	0,017*

SOFA: Sequential Organ Failure Assessment; qSOFA: quick Sepsis-related Organ Failure Assessment; NRL: Neutrophil-Lymphocyte Ratio; PLR: Platelet-Lymphocyte Ratio; LMR: Lymphocyte-to-Monocyte Ratio; CAR: C-reactive Protein-Albumin Ratio; AST: Aspartate Aminotransferase; ALT: Alanine Aminotransferase; *p<0,05 statistically significant.

A total of 46 patients had a low qSOFA score, and these patients were found to have a significantly shorter duration of hospitalization (p = 0.008).

Patients with a high CRP/Albumin Ratio (CAR) had a mean hospitalization time of 23.8 ± 3.8 days (range: 16.2–31.5), which was significantly longer (p = 0.05). Among the 29 patients with a high Neutrophil/Lymphocyte Ratio (NLR), eight died, and the mean hospitalization time was 23.6 ± 2.9 days (range: 17.8–29.4), also significantly prolonged (p = 0.03). **Table 3** summarizes the patients' mean laboratory findings measured at the time of admission and during hospitalization.

Table 3. Laboratory findings and mean hospital stays of patients with Covid-19 pneumonia patients

Laboratory findings	Number of patients	Mean hospital stay	P value
Lymphocytes,x10^9/ml			0,18
<800	17	21,7±3(15-28,5)	
>800	43	16±2(12-20)	
Platelets,x10^9/ml			0,15
<100.000	13	21±2,7(15-26)	
>100,000	47	17±2(1,9-21)	
CRP,mg/dl			0,001*
<50	21	11±1,3(9-14,4)	
>50	29	22,5±2,7(17-28)	
D-dimer,ng/ml			0,57
≤1000	51	17,9±2(14-22)	
>1000	9	18±2,9(12,4-23,8)	
Ferritin,ml/ng			0,07
<500	44	16,3±2(12-20,4)	
>500	16	23,3±3,5(16-30,2)	

CRP: C-reactive Protein-Albumin Ratio. *p<0,05 statistically significant

Sex, age, platelet count, lymphocyte count, ferritin levels, and D-dimer levels were not found to have a significant impact on mortality or total hospitalization time.

Discussion

This is a prospective study designed to evaluate the efficacy of serum ADMA levels—an indicator of endothelial dysfunction—in predicting length of hospital stay, thrombosis, and mortality in patients hospitalized with COVID-19 pneumonia.

Deaths associated with COVID-19 pneumonia have been reported at varying rates, ranging from 16% to 78% across different studies. A large study involving 20,133 patients reported an in-hospital mortality rate of 26% for those in general wards, with even higher rates among patients treated in intensive care units (ICUs) (9). In our study, the mortality rate was found to be 21%, which is consistent with findings in the existing literature.

ADMA is an endogenous inhibitor of nitric oxide (NO) synthesis. Its accumulation leads to inhibition of NO-mediated vasodilation, resulting in endothelial dysfunction. Elevated ADMA levels have been identified as an independent risk factor for cardiovascular diseases. A comprehensive meta-analysis involving 19,842 patients across 22 studies found a significantly increased risk of coronary artery disease and stroke in individuals with high ADMA levels (10). Additionally, several studies have shown that elevated ADMA levels are associated with increased short- and long-term mortality in critically ill patients (11).

The primary site of infection in COVID-19 pneumonia is the upper and lower respiratory tract. The relationship between respiratory tract diseases and ADMA levels has been explored in

several studies. In 2017, Vögeli et al. investigated the association between ADMA levels and mortality in 268 patients with community-acquired pneumonia (12). They found that ADMA levels were not a strong predictor of 30-day mortality (p = 0.086). However, elevated ADMA levels were associated with long-term mortality over a six-year follow-up, though this correlation was largely attributed to comorbidities and advanced age. Additionally, ADMA, a known nitric oxide synthase (NOS) inhibitor, has been detected in the sputum of patients with chronic obstructive pulmonary disease (COPD), another respiratory tract condition (13).

Only one study in the literature has examined the relationship between ADMA levels, mortality, and organ failure in patients diagnosed with COVID-19 pneumonia. This was a retrospective study involving just 31 patients, and it did not specify whether the patients had pneumonia. Serum ADMA concentrations were measured at admission, and levels were found to be higher in the 9 patients who died compared to those who survived (14). Notably, 16 of the patients in that study were diagnosed with COVID-19 pneumonia at other centers and referred to the study center only after requiring mechanical ventilation. The time interval between COVID-19 diagnosis and the development of respiratory failure was not clearly reported. Furthermore, only 15 patients were included at the time of diagnosis. Despite this, ADMA levels at admission were relatively low. n contrast, our study was a prospective investigation specifically involving patients diagnosed with COVID-19 pneumonia. Serum ADMA concentrations were measured in 60 patients using blood samples collected at the time of hospital admission. In our findings, ADMA levels were significantly lower in patients with COVID-19 pneumonia compared to the control group (p = 0.042). However, no significant relationship was observed between ADMA levels and length of hospital stay.

Low ADMA levels were first reported in 2003 in blood samples of 25 mice with endotoxemia (15). Subsequently, a prospective study involving 17 healthy young volunteers without comorbidities showed a decrease in serum ADMA levels 3.5 hours after injection of *Escherichia coli* (16). In our study, blood samples were collected within hours of diagnosis and stored under appropriate conditions. These findings suggest that ADMA levels in infection-related conditions may vary depending on the stage of the disease, with levels potentially being lower in the early phase.

The pathogenesis of COVID-19 has not yet been fully clarified. In patients admitted to intensive care units (ICUs), the primary cause of death is often related to viral sepsis. Some studies have reported a relationship between the severity of sepsis and plasma ADMA levels, while others have not found significant associations (17). A prospective study conducted in 2012 involving 27 ICU patients with septic shock and 17 with cardiogenic shock found no correlation between in-hospital mortality and ADMA levels measured at ICU admission (18). In contrast, another prospective study involving young ICU patients with sepsis reported lower ADMA levels on the first day of admission compared to healthy volunteers (19). The lack of serious comorbidities in this younger patient group was a notable strength, as it excluded additional risk factors known to elevate ADMA levels—such as kidney failure, atherosclerosis, and liver dysfunction—which are more common in older populations.

In patients with COVID-19 pneumonia, D-dimer, ferritin, C-reactive protein (CRP), and lactate dehydrogenase (LDH) levels measured

at admission were significantly elevated compared to the control group, consistent with findings in the literature (20). Natural killer (NK) cells and cytotoxic T lymphocytes play a critical role in the immune response to viral infections. Recent studies have shown that patients with severe COVID-19 pneumonia often present with lymphopenia, and lymphocyte levels are significantly lower in patients who succumb to the disease compared to survivors (21). In our study, lymphocyte counts were also significantly lower in COVID-19 patients compared to the control group ($p = 0.004$), and patients with lymphopenia had a longer duration of hospitalization.

Another aim of this study was to investigate the relationship between ADMA levels and thrombosis in patients with COVID-19 pneumonia, given that ADMA is a key marker of vascular endothelial dysfunction and is associated with atherosclerosis. Among the 60 patients included in the study, one developed acute ischemic cerebrovascular disease during hospitalization, while another developed lower extremity arterial thrombosis, underwent peripheral angiography, and subsequently received a stent. Both of these patients died during hospitalization. A third patient was treated for a left iliac arterial thrombus one month after discharge. In total, three patients experienced a thrombotic event. Due to the small number of such cases, a meaningful statistical relationship between ADMA levels and thrombosis could not be established.

The SOFA score is commonly used as a prognostic tool to assess organ dysfunction in critically ill patients, including those with chronic liver disease, hematological malignancies, and other severe conditions (22). In the context of COVID-19 pneumonia, several studies have demonstrated the prognostic value of the SOFA score, with a mean score of 2 reported among patients who later died (23, 24). Our study specifically focuses on a subset of COVID-19 patients with pneumonia—a group that holds a distinct clinical profile within the broader COVID-19 population. The mean SOFA score calculated at the time of hospital admission for all patients in our cohort was 2.43 ± 1.5 (range: 0–6), slightly higher than values reported in the literature. This elevated score was expected, given the severity of illness in this pneumonic subgroup. Among patients who later required intensive care, the mean ICU SOFA score was 5.18 ± 3.2 (range: 2–14), supporting findings by Raschke et al. in ICU patients requiring mechanical ventilation (25). These results suggest that initial SOFA scores may be insufficient for long-term prognostic assessment, as the clinical condition and laboratory parameters of patients evolve over time. Serial measurements may provide more meaningful insights into disease progression and outcomes.

In our study, consistent with the findings of Liu et al., patients with a qSOFA score of 1 or higher exhibited increased mortality rates (26). Notably, all patients in our cohort who had a high qSOFA score (≥ 1) at the time of referral to the intensive care unit died ($p = 0.07$). Given that the qSOFA score can be quickly and easily calculated at the bedside without the need for laboratory tests, it should be considered a valuable prognostic tool—especially during the COVID-19 pandemic, which has placed a significant burden on emergency services.

C-reactive protein (CRP), an acute-phase reactant, has been reported to increase in cases of COVID-19 pneumonia and may serve as an early predictor of severe infection—even before radiological findings are evident on CT scans (27). In our study, elevated CRP levels at the time of referral were significantly associated with prolonged hospitalization. Another pa-

rameter that showed a significant association with both hospitalization time and mortality was the CRP/albumin ratio (CAR). This finding is consistent with previous studies in the literature (28). Given that both CRP and albumin can be easily measured in most healthcare settings, these two parameters may serve as practical and accessible tools for predicting disease severity at the time of patient admission.

Recently, the Neutrophil/Lymphocyte Ratio (NLR), Platelet/Lymphocyte Ratio (PLR), and Monocyte/Lymphocyte Ratio (MLR) have been increasingly utilized as prognostic indicators in various inflammatory conditions. These ratios have shown potential as useful parameters in assessing disease progression and prognosis in patients with COVID-19 pneumonia as well.

In a retrospective analysis of clinical data from 443 COVID-19 pneumonia cases, Shang et al. reported that NLR, CRP, and platelet counts could aid in assessing disease severity, with NLR identified as the most reliable marker among them (29). The association between elevated NLR and increased disease severity in COVID-19 pneumonia has also been confirmed by other studies (30). In our study, although patients with low lymphocyte counts had longer hospitalization durations, this difference was not statistically significant. However, patients with higher NLR values exhibited both longer hospitalization times and higher mortality rates ($p = 0.03$). In contrast, PLR and MLR ratios were not effective in predicting prognosis in our patient cohort.

Limitations

The patient group included individuals with comorbidities known to increase plasma ADMA levels. Some studies have reported elevated ADMA levels, particularly in patients with active infections such as chronic obstructive pulmonary disease (COPD) (31). Despite the presence of comorbidities, ADMA levels in our patient group were lower than those in the control group. It is important to note that plasma ADMA levels were measured only once—using blood samples obtained at admission—and were not monitored during the follow-up period. Serial measurements could have provided insight into dynamic changes in ADMA levels over the course of the illness. Additionally, the number of patients who experienced thrombotic events was low, likely due to the limited sample size.

Conclusion

Serum ADMA concentrations measured in the early period of hospitalization were found to be significantly lower in patients with COVID-19 pneumonia compared to the control group. However, no correlation was observed between ADMA levels and length of hospital stay. Given the complex and not yet fully understood pathogenesis of COVID-19, larger prospective studies are needed to further evaluate the role of ADMA as a marker of endothelial dysfunction. COVID-19 pneumonia cases requiring ICU admission continue to have high mortality rates. Therefore, assessing the degree of organ dysfunction is essential when making decisions about hospitalization and ICU referral. It is important to recognize that patients with a SOFA score ≥ 3, qSOFA score ≥ 1, CRP/Albumin ratio ≥ 30, and Neutrophil/Lymphocyte Ratio ≥ 5 are at high risk of mortality and require early and aggressive clinical intervention.

References

1. Wu C., Chen X., Cai Y., et al. Risk Factors associated with acute respiratory distress syndrome and death in patients with coronavirus disease 2019 pneumonia in Wuhan, China. JAMA Intern Med 2020; 180(7):934-43. Doi: 10.1001/jamainternmed.2020.0994.
2. Hamming I., Bulthuis M.L.C., Lely A.T. Tissue distribution of ACE2 protein, the functional receptor for SARS coronavirus. A first step in understanding SARS pathogenesis. J Pathol 2014; 203(2):631–7. Doi:10.1002/path.1570.
3. Guan Wei-jie., Zheng-Yi N., Yu Hu., et al. Clinical characteristics of coronavirus disease2019 in China. New Engl J Med 2020; 382(18):1708–20. Doi:10.1056/NEJMoa2002032.
4. Varga Z., Flammer AJ., Steiger P., et al. Endothelial cell infection and endotheliitis in COVID-19. Lancet 2020; 395(10234):1417-8. Doi:10.1016/S0140-6736(20)30937-5.
5. Dowsett L., Higgins E., Alanazi S., Alshuwayer N.A., Leiper F.C., Leiper J. ADMA: A key player in the relationship between vascular dysfunction and inflammation in atherosclerosis. J Clin Med 2020; 9(9):3026. Doi:10.3390/jcm9093026.
6. Kang S., Tanaka T., Narazaki M. Targeting interleukin-6 signaling in clinic. Immunity 2019; 50(4):1007-23. Doi:10.1016/j.immuni.2019.03.026.
7. Freund Y., Lemachatti N., Krastinova E., et al. Prognostic accuracy of sepsis-3 criteria for in-hospital mortality among patients with suspected infection presenting to the emergency department. JAMA 2017; 317(3):301–8. Doi:10.1001/jama.2016.20329.
8. Vincent JL., Mendonça A., Cantraine F., et al. Use of the SOFA score to assess the incidence of organ dysfunction/failure in intensive care units: results of amulticenter, prospective study. Working group on "sepsis-related problems" of the European Society of Intensive Care Medicine. Crit Care Med 1998; 26(11):1793–800. Doi:10.1097/00003246-199811000-00016.
9. Docherty AB., Harrison EM., Green CA., et al. Features of 20 133 UK patients in hospital with covid-19 using the ISARIC WHO clinical characterisation protocol: prospective observational cohort study. BMJ 2020; 369(22):1985. Doi:10.1136/bmj.m1985.
10. Willeit P., Freitag DF., Laukkanen JA., et al. Asymmetric dimethylarginine and cardiovascular risk: systematic review and meta-analysis of 22 prospective studies. J Am Heart Assoc 2015; 4(6):e001833. Doi:10.1161/JAHA.115.001833.
11. Koch A., Weiskirchen R., Kunze J., et al. Elevated asymmetric dimethylarginine levels predict short- and long-term mortality risk in critically ill patients. J Crit Care 2013; 28(6):947-53. Doi:10.1016/j.jcrc.2013.05.016.
12. Vögeli A., Ottiger M., Meier MA., et al. Admission levels of asymmetric and symmetric dimethylarginine predict long-term outcome in patients with community-acquired pneumonia. Respir Res 2017 ;18(1):25. Doi:10.1186/s12931-017-0502-4.
13. Scott J.A., Duongh M., Young A.W., Subbarao P., Gauvreau G.M., Grasemann H. Asymmetric dimethylarginine in chdavironic obstructive pulmonary disease (ADMA in COPD). Int J Mol Sci 2014; 15(4):6062-71. Doi:10.3390/ijms15046062.
14. Hannemann J., Balfanz P., Schwedhelm E., et al. Elevated serum SDMA and ADMA at hospital admission predict in-hospital mortality of COVID-19 patients. Sci Rep 2021; 11(1):9895. Doi:10.1038/s41598-021-89180-w.
15. Robert J.N., Tom T., Coen van G., et al. Handling of asymmetrical dimethylarginine and symmetrical dimethylarginine by the rat kidney under basal conditions and during endotoxaemia. Nephrol Dial Transplant 2003; 18(12):2542-50. Doi:10.1093/ndt/gfg452.
16. Mittermayer F., Namiranian K., Pleiner J., Schaller G., Wolzt M. Acute escherichia coli endotoxaemia decreases the plasma l-arginine/asymmetrical dimethylarginine ratio in humans. Clin Sci (Lond) 2004; 106(6):577–81. Doi:10.1042/CS20030363.
17. Winkler MS., Nierhaus A., Rösler G., et al. Symmetrical (SDMA) and asymmetrical dimethylarginine (ADMA) in sepsis: high plasma levels as combined risk markers for sepsis survival. Crit Care 2018; 22(1):216. Doi:10.1186/s13054-018-2090-1.
18. Visser M., Vermeulen MA., Richir MC., et al. Imbalance of arginine and asymmetric dimethylarginine is associated with markers of circulatory failure, organ failure and mortality in shock patients. Br J Nutr 2012; 107(10):1458-65. Doi:10.1017/S0007114511004648.
19. Weiss S.L., Haymond S., Ralay Ranaivo H., et al. Evaluation of asymmetric dimethylarginine, arginine, and carnitine metabolism in pediatric sepsis. Pediatr Crit Care Med 2012; 13(4):e210-8. Doi:10.1097/PCC.0b013e318238b5cd.

20. Terpos E., Ntanasis-Stathopoulos I., Elalamy I., et al. Hematological findings and complications of COVID-19. Am J Hematol 2020; 95(7):834-47. Doi:10.1002/ajh.25829.
21. Ruan Q., Yang, K., Wang, W., et al. Clinical predictors of mortality due to COVID 19 based on an analysis of data of 150 patients from Wuhan, China. Intensive Care Med 2020; 40(5):846–8. Doi:10.1007/s00134-020-06028-z.
22. Cetintepe T., Cetintepe L., Solmaz S., et al. Determination of the relationship between mortality and SOFA, qSOFA, MASCC scores in febrile neutropenic patients monitored in the intensive care unit. Support Care Cancer 2021; 29(7):4089-94. Doi:10.1007/s00520-020-05924-w.
23. Vaquero-Roncero LM., Sánchez-Barrado E., Escobar-Macias D., et al. C-Reactive protein and SOFA scale: A simple score as early predictor of critical care requirement in patients with COVID-19 pneumonia in Spain. Rev Esp Anestesiol Reanim (Engl Ed) 2021; 68(9):513-22. Doi:10.1016/j.redare.2020.11.008.
24. Yang Z., Hu Q., Huang F., Xiong S., Sun Y. The prognostic value of the SOFA score in patients with COVID-19: A retrospective, observational study. Medicine (Baltimore) 2021; 13:100(32):e26900. Doi:10.1097/MD.0000000000026900.
25. Raschke RA., Agarwal S., Rangan P., Heise C.W., Curry S.C. Discriminant accuracy of the SOFA score for determining the probable mortality of patients with COVID-19 pneumonia requiring mechanical ventilation. JAMA 2021; 325(14):1469-70. Doi:10.1001/jama.2021.1545.
26. Liu S., Yao N., Qiu Y., He C. Predictive performance of SOFA and qSOFA for in-hospital mortality in severe novel coronavirus disease. Am J Emerg Med 2020; 38(10):2074–80. Doi:10.1016/j.ajem.2020.07.019.
27. Tan C., Huang Y., Shi F., et al. C-reactive protein correlates with computed tomographic findings and predicts severe COVID-19 early. J Med Virol 2020; 92(7):856-62. Doi:10.1002/jmv.25871.
28. Karakoyun I., Colak A., Turken M., et al. Diagnostic utility of C-reactive protein to albumin ratio as an early warning sign in hospitalized severe COVID-19 patients. Int Immunopharmacol 2021; 91:107285. Doi:10.1016/j.intimp.2020.107285.
29. Shang W., Dong J., Ren Y., et al. The value of clinical parameters in predicting the severity of COVID-19. J Med Virol 2020; 92(10):2188-92. Doi:10.1002/jmv.26031.
30. Calim A., Yanic U., Halefoglu A.M., et al. Is there a relationship between epicardial adipose tissue, inflammatory markers, and the severity of COVID-19 pneumonia? Sisli Etfal Hastan Tip Bul 2023; 57(3):387-96. Doi: 10.14744/SEMB.2023.99582.
31. Ozkarafakili MA., Kara ZMY., Serin E. Asymmetric dimethylarginine in COPD Exacerbation. Med Bull Sisli Etfal Hosp 2022; 56(4):536-42. Doi:10.14744/SEMB.2022.23682.

INVESTIGATION OF MANDIBULAR CONDYLE SHAPE IN PEDIATRIC POPULATION ACCORDING TO AGE AND GENDER INVESTIGATION OF THE CONDYLE HEAD SHAPE

PEDİATRİK POPULASYONDA MANDİBULAR KONDİL ŞEKLİNİN YAŞ VE CİNSİYETE GÖRE ARAŞTIRILMASI KONDİL BAŞI ŞEKLİNİN İNCELENMESİ

Mehmet UNAL*[1], Ozan TURAMANLAR[2]

[1]Afyonkarahisar Health Sciences University, Faculty of Dentistry, Department of Pedodontics Afyonkarahisar, Türkiye. e-mail: mehmet.unal@afsu.edu.tr
[2]Izmir Kâtip Çelebi University, Faculty of Medicine, Department of Anatomy, Izmir, Türkiye, e-mail: ozanturamanlar@hotmail.com

ORCID ID: MU: 0000-0001-9111-6962 **OT:** 0000-0002-0785-483X

DOI: 10.52818/cjmr.1648327 **E-ISSN:** 2791-7061

ARTICLE INFO

Article Information

Article Type:
Research Article
Received: 28.02.2025
Accepted: 19.04.2025
Published: 30.04.2025

Keywords:
Condylar head,
Condylar process,
Mandibular condyle types,
Pediatric populations

ABSTRACT

Objective: The mandibular condyle is a key anatomical landmark involved in facial growth. The temporomandibular joint (TMJ), which plays a crucial role in mastication and speech, is of significant interest to dentists, orthodontists, clinicians, and radiologists. This study aims to document the normal morphological variations of the condyle using panoramic radiographs in pediatric populations.

Materials and Methods: The present study involved the radiographic evaluation of 400 condylar heads from 200 patients, comprising 101 females (50.5%) and 99 males (49.5%), aged between 6 and 12 years. Five types of condylar morphology were identified: (a) bird beak, (b) diamond, (c) oval, (d) crooked finger, and (e) smooth-shaped.

Results: A total of 133 patients were classified under the Diamond category. In the Oval category, the measurements of the right and left condyles were found to be similar. The remaining categories, in descending order of frequency, were Smooth, Cooked Finger, and Bird Beak. A statistically significant difference ($p < 0.05$) was observed between the left and right side measurements in female patients.

Conclusions: We believe that increasing the sample size and incorporating three-dimensional evaluations will enhance the understanding of anatomical structures in this region. Future studies utilizing panoramic images reconstructed from three-dimensional data are needed to determine whether they can overcome the limitations associated with conventional and digital panoramic imaging. A comprehensive understanding of the morphological variations in mandibular condyle configuration is essential for distinguishing normal anatomical variants from pathological conditions.

MAKALE BİLGİLERİ

Makale Bilgisi

Makale Türü:
Araştırma Makalesi
Geliş Tarihi: 28.02.2025
Kabul Tarihi: 19.04.2025
Yayım Tarihi : 30.04.2025

Anahtar Kelimeler:
Kondil başı,
Kondiler proses,
Mandibular kondil tipleri,
Pediatrik popülasyon

ÖZET

Amaç: Mandibular kondil, yüz büyümesi için önemli bir anatomik dönüm noktasıdır. Temporomandibular eklemin (TME) en önemli fonksiyonları çiğneme ve konuşmadır ve diş hekimleri, ortodontistler, klinisyenler ve radyologlar için büyük ilgi çekicidir. Bu çalışmanın amacı, pediatrik popülasyonlarda panoramik radyografiler aracılığıyla kondilin farklı tipteki normal morfolojik varyasyonlarının belgelenmesidir.

Gereç ve Yöntemler: Bu çalışma, 6-12 yaş arası 101'i (%50,5) kız ve 99'u (%49,5) erkek olmak üzere 200 kişinin görüntülenmesinin ardından 400 kondil başının radyolojik değerlendirmesini içermektedir. Beş tip kondiler morfoloji tanımlanmıştır: a)Kuş gagası, b) Elmas, c) Oval, d) Açılı, e) Düzgün şekilli.

Bulgular: Elmas kategorisine toplam 133 kişi tespit edildi. Oval kategorisinde sağ ve sol taraftaki ölçümlerin simetrik (benzer) olduğu görülmüştür. Diğer kategoriler Elmas, Düz, Açılı ve Kuş Gagasıdır. Kızlarda sol ve sağ taraf ölçüm kategorileri arasındaki fark istatistiksel olarak anlamlı bulunmuştur. ($p<0,05$).

Sonuç: Örneklem sayısının arttırılması ve üç boyutlu değerlendirmelerin yapılmasının bu bölgedeki anatomik yapıların tanımı ve değişimini netleştirmeye yardımcı olacağına inanıyoruz. Konvansiyonel ve dijital panoramik görüntülerin kısıtlamalarının üstesinden gelip gelmediklerini belirlemek için 3 boyutlu verilerden oluşturulan panoramik görüntüleri kullanan çalışmalara ihtiyaç vardır. Mandibular kondil şeklindeki morfolojik varyasyonların kapsamlı bir şekilde bilinmesi, standart bir varyant ile anormal bir durumu ayırt etmek için hayati önem taşımaktadır.

Unal M., Turamanlar O. Investigation of Mandibular Condyle Shape in Pediatric Population According to Age and Gender. CJMR 2025; 5(1):12-21
Correspondence to: Mehmet UNAL, Afyonkarahisar Health Sciences University, Faculty of Dentistry, Department of Pedodontics Afyonkarahisar, Turkey
Authorship Contributions: For the preparation of the article all authors have taken equal responsibility. All authors discussed the results and contributed to the final manuscript
Conflict of Interest: The authors declare that they have no conflict of interest.
Acknowledgement: We would like to thank Specialist Zeynep Uzel for her help in the statistical phase of this study.
Ethics Approval: This retrospective study was approved by the Afyonkarahisar Health Sciences University Clinical Research Ethics Committee (Approval No: 2023/494).

Introduction

The temporomandibular joint (TMJ) is one of the most complex joints in the human body. It connects the mandible to the skull and functions bilaterally and simultaneously. The TMJ comprises several key anatomical components: the mandibular condyle, the mandibular fossa, and the articular eminences of the temporal bone, along with the soft tissue structures including the articular disc, its attachments, and the joint cavity (1).

The temporomandibular joint (TMJ), also known as the mandibular joint, is a bicondylar joint with an ellipsoid shape (2). Compared to other diarthrodial joints, the TMJ is considerably underdeveloped at birth, making it vulnerable to perinatal and postnatal insults. The joint continues to develop during early childhood as the jaw is engaged in sucking motions and, later, in chewing (3). The TMJ plays a critical role in mastication and speech and is of significant interest to dentists, orthodontists, clinicians, and radiologists (4).

The mandibular condyle is a key anatomical landmark essential for facial growth (5). It can exhibit developmental variations as part of its adaptation to pathological conditions, developmental abnormalities, and remodeling processes (6).

Changes in the morphology of the mandibular condyle can arise from various causes, including infections, trauma, tumors, condylar hyperplasia, and ankylosis (7). The shape of the mandibular condyle has been extensively evaluated in previous studies, with considerable variation reported (8). Most morphological changes have been observed in the elderly, primarily due to degenerative alterations in the joint.

The appearance of the mandibular condyle can vary significantly between individuals and across age groups (3). A thorough understanding of the anatomy and morphology of the entire temporomandibular joint (TMJ) is essential for distinguishing normal developmental variations from pathological conditions. The "mixed dentition" period is particularly critical, as any developmental changes during this stage can affect the occlusal relationship of the permanent dentition, which persists throughout life. During this period, various dentocraniofacial anomalies may arise. These anomalies may resolve spontaneously with continued growth and development or, if persistent, may require timely intervention to prevent further complications (9).

Limited data are available on the morphological appearance of the mandibular condyle in pediatric populations. A thorough understanding of its morphological variations is essential for distinguishing normal anatomical variants from pathological conditions. This study aims to document the different types of normal morphological variations of the condyle using panoramic radiographs in pediatric patients.

Materials and Methods

This retrospective study was approved by the Afyonkarahisar Health Sciences University Clinical Research Ethics Committee (Approval No: 2023/494). The cross-sectional study was conducted at the Afyonkarahisar Health Sciences University Faculty of Dentistry, Department of Pediatric Dentistry. A total of 400 condylar heads were radiographically evaluated from 200 digitized orthopantomograms (OPGs). All available OPGs of individuals who visited the department between October 2023 and December 2023 were retrieved from the faculty archive, along with relevant demographic information including age and gender.

The inclusion criteria for the study were as follows:

i) panoramic radiographs of patients aged 6–12 years with available demographic information (age and gender);

ii) radiographs displaying a full view of either side of the mandible with optimal density and contrast; and

iii) absence of projection errors that could distort the image.

Panoramic radiographs were excluded from the study if they exhibited any pathology in the maxilla or mandible; evidence of mandibular fractures; developmental anomalies of the jaws; craniofacial syndromes; previous plating for fractures; presence of odontogenic cysts or tumors; complete dentures; or edentulous dental arches.

All radiographs were obtained using the same machine (Planmeca ProMax 2D, Finland) at Afyonkarahisar Health Sciences University, Faculty of Dentistry. The panoramic radiographs were collected in printed format using the Planmeca Romexis software. Five distinct types of condylar morphology were identified: (a) bird beak, (b) diamond, (c) oval, (d) crooked finger, and (e) smooth-shaped (Figure 1).

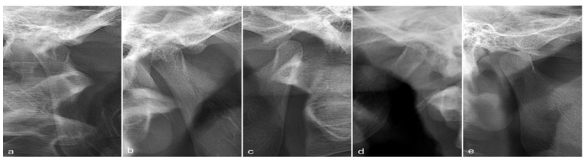

Figure 1: *Shapes of condyle; a)Bird Beak, b) Diamond, c) Oval, d) Cooked Finger, e) Smooth*

The study included 200 patients, comprising 101 females (50.5%) and 99 males (49.5%) between the ages of 6 and 12 years. The mean age of the patients was 8.86 ± 2.06 years (Tables 1 and 2).

Table 1: *Descriptive Statistics of Patients*

	Statistics
Sex, *n* (%)	
Female	101 (%50.5)
Male	99 (%49.5)
Age	8.86±2.06
Right, *n* (%)	
Bird Beak	17 (%8.5)
Diamond	134 (%67)
Oval	28 (%14)
Cooked Finger	5 (%2.5)
Smooth	16 (%8)
Left, *n* (%)	
Bird Beak	9 (%4.5)
Diamond	133 (%66.5)
Oval	23 (%11.5)
Cooked Finger	17 (%8.5)
Smooth	18 (%9)
Total	200 (%100)

Table 2: *Comparison of Right and Left Side Measurement Categories*

			Right					Total	Test Statistics	p
			Bird Beak	Diamond	Oval	Cooked Finger	Smooth			
Left	Bird Beak	n	6_a	1_b	1_b	$0_{a,b}$	1_b	9	**20.091**	**0.010**
		%	66.7%	11.1%	11.1%	0.0%	11.1%	100.0%		
	Diamond	n	$9_{a,b}$	96_b	$18_{a,b}$	1_a	$9_{a,b}$	133		
		%	6.8%	72.2%	13.5%	0.8%	6.8%	100.0%		
	Oval	n	0_a	18_a	4_a	0_a	1_a	23		
		%	0.0%	78.3%	17.4%	0.0%	4.3%	100.0%		
	Cooked Finger	n	0_a	12_a	1_a	4_b	0_a	17		
		%	0.0%	70.6%	5.9%	23.5%	0.0%	100.0%		
	Smooth	n	$2_{a,b}$	7_b	$4_{a,b}$	$0_{a,b}$	5_a	18		
		%	11.1%	38.9%	22.2%	0.0%	27.8%	100.0%		
Total %		n	17	134	28	5	16	200		
		8.5%	67.0%	14.0%	2.5%	8.0%	100.0%			

The application of line based labeling, where different letters in the same line indicate a statistical difference.

Statistics

Data analysis was performed using IBM SPSS Statistics Standard Concurrent User Version 26 (IBM Corp., Armonk, NY, USA). Descriptive statistics were presented as frequency (n), percentage (%), and mean ± standard deviation. The relationships between dependent categorical variables were assessed using the McNemar test. A p-value of <0.05 was considered statistically significant.

Multiple correspondence analysis is a simple correspondence analysis extended to the case of the categorical variable Q and performed on the indicator matrix of the data. Suppose the variable q has jq categories and the sum of the categories is $J = \sum J_q$. N units, then the indicator matrix Z becomes an nxJ dimensional matrix of zeros and ones.

In the analysis of the indicator matrix Z, the total variation becomes the chi-squared statistic, calculated like a contingency table over Z, and is defined as $\chi_z^2 = n(J - Q)$.

The indicator matrix is denoted as Z $\equiv [Z_1 \ldots . Z_Q]$ and shows the categories and the categorical variable $Z_q(nxJ_q), J_q$. Since the Burt matrix B is symmetric, it can be shown that the optimal column parameters during the fitness analysis of the indicator matrix Z are similar to the row or column parameters during the analysis of the Burt matrix B. The principal inertias (μ_k^2 components) of matrix B are the squares of those in the indicator matrix Z. In this way, once B is found, the solution for the columns (categories) of Z can be provided within the multiple correspondence analysis. Although the indicator matrix Z covers the multidirectional information contained in the data, it is clear that the multiple correspondence analysis analyses only two-way information. Consequently, it can be said that the multiple correspondence analysis is a weighted least squares approximation of

the Burt matrix. The chi-squared statistic can be recalculated like a contingency table for B. It can be simplified as follows:

$$\chi_B^2 = \sum\sum_{q \neq s} \chi_{qs}^2 + n(J - Q) \quad (1)$$

Here, χ_{qs}^2, represents the chi-square statistic for the sub-table $N_{qs}^2 = Z_q' Z_s$ of non-diagonal elements. Total Variation is measured as the sum of the following $\sum\sum_{q \neq s} \chi_{qs}^2$.

Given a Burt matrix B, multi-fitness analysis can be defined as a least-squares approximation of B with a lower-rank matrix H that minimises the equation.

$$b^{-1tr}\left\{D_r^{-1}(B-H)D_r^{-1}(B-H)'\right\} \quad (2)$$

This is a suitability analysis of the Burt matrix B. The b here is the grand sum of matrix B. Dr, on the other hand, is the diagonal matrix of row and column category proportions, since matrix B is symmetric. Each sub-table Nqs can be expressed as $b = NQ^2$ the total number of units n of the Burt matrix B as far as n is transformed into a crosstabulation. For variable q, the vector of category proportions Jq is denoted by rq, (1'rq = 1). This is also the set of row category proportions Nqs for any s. The Jq × Jq dimension is denoted by Dq, a diagonal matrix composed of q r elements. In this context, the equation can be rewritten as follows:

$$n^{-1}tr\left\{D_r^{-1}(B-H)D_r^{-1}(B-H)'\right\} =$$
$$n^{-1}\sum_{q=1}^{Q}\sum_{s=1}^{Q}\left\{D_q^{-1}(N_{qs}-H_{qs})D_s^{-1}(N_{qs}-H_{qs})'\right\} \quad (3)$$

Here, the supermatrix of Hqs is represented by H.

$$\left\|N_{qs}-H_{qs}\right\|_{qs}^2 = tr$$

In this case, $\left\{D_q^{-1}(N_{qs}-H_{qs})D_s^{-1}(N_{qs}-H_{qs})'\right\}$, The equation (3), can be written in a simpler form as follows:

$$n^{-1}\sum_q\sum_s\left\|N_{qs}-H_{qs})'\right\|_{qs}^2 \quad (4)$$

The function minimized by this method is:

$$n^{-1}\sum_q\sum_{q<s}\left\|N_{qs}-H_{qs})'\right\|_{qs}^2 \quad (5)$$

The sum of the term $\frac{1}{2}Q(Q-1)$ corresponds to the sub-table of elements above the diagonal elements of B. The minimisation of the equation (3) is equal to the minimisation of the inconsistency function defined by Healy & Goldstein (10) and the internal consistency criterion defined by Nishisato (11).

Results

A total of 9 patients were classified under the Bird Beak category based on left-side condylar measurements. Within this group, 66.7% remained in the Bird Beak category on the right side, while 11.1% shifted to the Diamond category, 11.1% to the Oval category, and 11.1% to the Smooth category. A statistically significant difference was observed between the Bird Beak category and the Diamond, Oval, and Smooth categories ($p < 0.05$).

A total of 133 patients were classified under the Diamond category. Among these patients, 6.8% were found in the Bird Beak category, 72.2% remained in the Diamond category, 13.5% in the Oval category, 0.8% in the Cooked Finger category, and 6.8% in the Smooth category on the contralateral side. A statistically significant difference was observed between the Diamond and Cooked Finger categories ($p < 0.05$).

A total of 17 patients were classified under the Cooked Finger category. A statistically significant difference was observed between the Cooked Finger category and all other condylar morphology categories ($p < 0.05$). Additionally, 18 patients were included in the Smooth category, and a significant difference was found

between the Smooth and Diamond categories.

The differences between left-sided and right-sided condylar morphology categories were analyzed according to gender. A statistically significant difference was observed between the left and right sides in female patients (p<0.05) (Table 3).

Table 3: *Comparison of Right and Left Side Measurement Categories by Gender*

Right										
			Bird Beak	Diamond	Oval	Cooked Finger	Smooth	Total	Test statistics	p
Female	Bird Beak	n	3_a	0_b	0_b	0_b	1_c	4	**14.726**	**0.023**
		%	75.0%	0.0%	0.0%	0.0%	25.0%	100.0%		
	Diamond	n	$5_{a,b}$	$41_{a,b}$	13_b	1_a	2_a	62		
		%	8.1%	66.1%	21.0%	1.6%	3.2%	100.0%		
	Oval	n	0_a	12_a	2_a	0_a	0_a	14		
		%	0.0%	85.7%	14.3%	0.0%	0.0%	100.0%		
	Cooked Finger	n	0_a	9_a	0_a	3_b	0_a	12		
		%	0.0%	75.0%	0.0%	25.0%	0.0%	100.0%		
	Smooth	n	0_a	5_a	1_a	$0_{a,b}$	3_b	9		
		%	0.0%	55.6%	11.1%	0.0%	33.3%	100.0%		
	Total %	n	8	67	16	4	6	101		
		%	7.9%	66.3%	15.8%	4.0%	5.9%	100.0%		
Male	Bird Beak	n	3_a	1_b	$1_{a,b}$	$0_{a,b}$	0_b	5	12.669	0.124
		%	60.0%	20.0%	20.0%	0.0%	0.0%	100.0%		
	Diamond	n	4_a	55_b	5_a	0_a	$7_{a,b}$	71		
		%	5.6%	77.5%	7.0%	0.0%	9.9%	100.0%		
	Oval	n	0_a	6_a	2_a	0_a	1_a	9		
		%	0.0%	66.7%	22.2%	0.0%	11.1%	100.0%		
	Cooked Finger	n	0_a	3_a	1_a	1_b	0_a	5		
		%	0.0%	60.0%	20.0%	20.0%	0.0%	100.0%		
	Smooth	n	2_a	2_b	3_a	$0_{a,b}$	2_a	9		
		%	22.2%	22.2%	33.3%	0.0%	22.2%	100.0%		
	Total	n	9	67	12	1	10	99		
		%	9.1%	67.7%	12.1%	1.0%	10.1%	100.0%		

The application of line based labeling, where different letters in the same line indicate a statistical difference.

Among female patients, a total of 4 were classified under the Bird Beak category based on left-side measurements. A statistically significant difference was observed between the Bird Beak category and the Smooth, Diamond, Oval, and Cooked Finger categories (p < 0.05).

A total of 62 patients were classified under the Diamond category in this part of the study. Among these, 8.1% were found in the Bird Beak category, 66.1% remained in the Diamond category, 21% were in the Oval category, 1.6% in the Cooked Finger category, and 3.2% in the Smooth category on the contralateral side. A statistically significant difference was observed between the

Oval category and both the Cooked Finger and Smooth categories ($p < 0.05$).

A total of 12 patients were classified under the Oval category. Among these, 85.7% had right-sided measurements in the Diamond category, while 14.3% had right-sided measurements in the Oval category. This distribution showed a statistically significant difference ($p < 0.05$).

A total of 12 patients were classified under the Cooked Finger category. Among these, 75% had right-sided measurements in the Diamond category, while 25% had right-sided measurements in the Cooked Finger category. A statistically significant difference was observed between the Cooked Finger category and all other condylar morphology categories ($p < 0.05$).

A total of 9 patients were classified under the Smooth category. Among them, 55.6% had right-sided measurements in the Diamond category, 11.1% in the Oval category, and 33.3% in the Smooth category. A statistically significant difference was observed between the Smooth category and all other categories, except for the Cooked Finger category ($p < 0.05$).

Table 4 presents the results of the indicator matrix analysis. Based on this analysis, the rank of the corresponding Burt matrix was determined to be 1. The "Inertia" column in Table 4 indicates the amount of variance (inertia) explained by each dimension, representing the average variation across the levels of the variables. Analysis of these values shows that the contributions of each dimension to the total inertia are relatively similar. The proportion of total variance explained by each dimension was calculated by comparing the inertia of each dimension to the total inertia. The first dimension accounted for the highest explanatory power at 56.2%, followed by the second dimension at 28.9%, yielding a combined explanation rate of 85.1%.

Table 4: *Initial Matrix Analysis Results*

Dimension	Proportion of Inertia		Confidence Singular Value	
	Accounted for	Cumulative	Standard Deviation	Correlation
1	0.562	0.562	0.026	0.571
2	0.289	0.851	0.029	
3	0.146	0.997		
4	0.003	1.000		
Total	1.000	1.000		

Although representing the relationships between the levels of these variables in a two-dimensional space is not sufficient to fully explain the overall variance, two dimensions were used for the purpose of visual interpretation. Table 5 presents the correlation coefficients between the dimensions, the contribution of each level to the respective dimensions, and their coordinates within the two-dimensional space.

As shown in Table 5, the Diamond category makes the largest individual contribution to Dimension 1. However, when the Oval and Diamond categories are considered together, they appear to contribute most significantly to both Dimension 1 and Dimension 2, depending on how they are grouped or ordered in the analysis.

Table 5: *Central Coordinates of Categories of Variables According to Dimensions*

Right	Mass	Score in Dimension		Inertia
		1	2	
Bird Beak	0.083	-1.977	0.977	0.196
Diamond	0.673	0.293	-0.100	0.041
Oval	0.139	-0.223	-0.324	0.014
Cooked Finger	0.029	1.660	2.787	0.135
Smooth	0.076	-0.676	-0.668	0.068
Active Total	1.000			0.453

According to Figure 2, based on the distanc-

es from the center—representing the overall mean configuration—the greatest symmetry between right and left condylar morphology is observed in the Oval category. In other words, when the condyle is classified as Oval, there is a high probability that the right and left measurements are similar, indicating strong bilateral agreement. This is followed by the Diamond and Smooth categories, with lower levels of agreement observed in the Cooked Finger and Bird Beak categories.

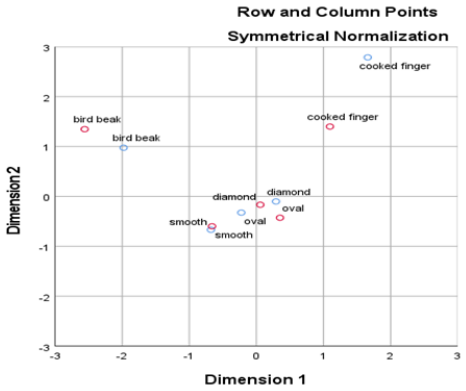

Figure 2: *Multiple Correspondence Analysis Graph*

Discussion

The American Academy of Oral and Maxillofacial Radiology recommends routine use of panoramic radiographs to evaluate the structural components of the temporomandibular joint (TMJ), due to their relatively low radiation exposure and cost compared to computed tomography (3).

Panoramic radiographs are the most commonly used diagnostic tool among dental clinicians, providing valuable information about the teeth, mandible, and associated jaw structures (3). Dentists and orthodontists widely regard panoramic radiography as the current standard of care for dental diagnosis and treatment planning, and it can also aid in the early detection of temporomandibular joint disorders (TMDs) (3, 12, 13). The mandibular condyle serves as a critical anatomical reference point in relation to facial growth, exhibiting considerable variation in shape and size across different age groups and individuals (3). Furthermore, the condylar process is a key anatomical component of the mandible, directing mandibular bone growth in both vertical and sagittal dimensions (14).

A comparative analysis of condylar head shape distributions across different dentition stages has shown that round-shaped condyles are most commonly observed during the primary dentition phase, while convex-shaped condyles are most prevalent during the permanent dentition phase. A transitional pattern from round to convex shapes is typically observed during the mixed dentition period (15). In comparison, the age group analyzed in our study falls within the mixed dentition phase; however, the Diamond-shaped condyle was the most frequently observed morphology in our dataset.

Shaikh et al. reported that oval-shaped condylar morphology was more frequently observed in males, whereas diamond-shaped morphology was more prevalent in females (3). In contrast, our study found that diamond-shaped condylar morphology was the most common in both male and female groups.

In a study by Al Saedi, the oval shape was reported as the most common form of the mandibular condyle in a young adult population, accounting for 56% of the total sample (8). Conversely, Ozbilen found that various non-oval condylar shapes became more prevalent with increasing age, likely due to heightened occlusal forces (16). In our study, which focused on a younger age group, the Diamond-shaped condyle was the most frequently observed morphology.

Singh et al. conducted a study on the normal morphology of mandibular condyles within a defined population and reported that the round-shaped morphology was the most prevalent, observed in 62% of the study population (1). He emphasized that the shape of the mandibular condyle can vary considerably and categorized it into four primary types: flat, pointed, angled, and round. Although a different classification system was employed in our study, we found that diamond-shaped condylar heads were more common than oval-shaped ones.

According to Khanai, the most common condylar shape observed in younger individuals was oval, whereas diamond-shaped condyles were more frequently seen in the older age group (17). This finding suggests that condylar morphology may change with age and can be influenced by various factors, including age, sex, occlusal forces, malocclusion, and skeletal classification. However, in the present study—despite the relatively young age of the participants—the Diamond-shaped condyle was identified as the most prevalent morphology.

The findings from the study by Tanu et al. demonstrate that the morphology of the condylar head undergoes notable changes during the mixed dentition period, with round-shaped condyles being more common in younger children and convex-shaped condyles becoming more prevalent as children approach the establishment of fully functional dentition (18). In our study, the Diamond-shaped condylar head—interpreted as a form of convex morphology—was the most frequently observed in the mixed dentition population. This discrepancy may be attributed to racial or ethnic differences, as the study by Tanu et al. was conducted in a Far Eastern population.

To our knowledge, there is a lack of sufficient studies examining the morphology of the mandibular condyle in a young and healthy Turkish pediatric population. Therefore, further research using cone beam computed tomography (CBCT), which allows for more detailed and accurate evaluation of condylar morphology, is recommended. The absence of CBCT imaging in our study may be considered a limitation.

Conclusions

In this study, the most common shapes of the mandibular condyle were examined using panoramic radiographs of patients in their developmental period. The diamond-shaped condyle was the most frequently observed in both sexes, accounting for approximately two-thirds of the sample. The Diamond–Diamond combination was the most common bilateral pattern. Further studies on Turkish pediatric populations—particularly those employing Cone Beam Computed Tomography (CBCT)—are warranted. Increasing the sample size and incorporating three-dimensional evaluations will aid in better defining and understanding the morphological variations and developmental changes in this anatomical region.

Limitations

One of the main limitations of our study is the inability to utilize cone-beam computed tomography (CBCT), which provides high-resolution three-dimensional imaging of anatomical structures. Additionally, the sample size was relatively limited, and future studies should include a larger population to enhance the generalizability of the findings.

Acknowledgement

We would like to express our sincere gratitude to Specialist Zeynep Uzel for her valuable assistance during the statistical phase of this study.

Founding sources

This research did not receive any specific grant from funding agencies in the public, commercial, or not-for-profit sectors.

References

1. Singh B., Kumar, N. R., Balan, A., et al. Evaluation of normal morphology of mandibular condyle: a radiographic survey. J Clin Imaging Sci 202; 10, 51. Doi: 10.25259/JCIS_84_2020.
2. Alomar X., Medrano J., Cabratosa J., et al. Anatomy of the temporomandibular joint. Semin Ultrasound CT MR 2007; 28(3):170–83. Doi: 10.1053/j.sult.2007.02.002.
3. Shaikh AH., Ahmed S., Ahmed AR., et al. Assessment of radiographic morphology of mandibular condyles: a radiographic study. Folia Morphol (Warsz) 2022; 81(2):481–6. Doi: 10.5603/FM.a2021.0049.
4. Bag AK., Gaddikeri S., Singhal A., et al. Imaging of the temporomandibular joint: an update. World J Radiol 2014; 6(8):567–82. Doi:10.4329/wjr.v6.i8.567.
5. Halicioglu K., Celikoglu M., Buyuk SK., Sekerci AE., Candirli C. Effects of early unilateral mandibular first molar extraction on condylar and ramal vertical asymmetry. Eur J Dent 2014; 8(2):178–83. Doi: 10.4103/1305-7456.130595.
6. Ahn SJ., Kim TW., Lee DY., Nahm DS. Evaluation of internal derangement of the temporomandibular joint by panoramic radiographs compared with magnetic resonance imaging. Am J Orthod Dentofacial Orthop 2006; 129(4):479–85. Doi: 10.1016/j.ajodo.2005.12.009.
7. Anisuzzaman M., Khan SR., Khan MTI., Abdullah MK., Afrin A. Evaluation of mandibular condylar morphology by orthopantomogram in Bangladeshi population. Update Dent Coll J 2019; 9(1):29–31. Doi: 10.3329/updcj.v9i1.41203.
8. Al-Saedi AIL., Riad AL., Al-Jasim NH., Bahaa AL. A panoramic study of the morphology of mandibular condyle in a sample of population from Basrah city. Int J Morphol 2020; 38(6):1707-12. Doi: 10.4067/S0717-95022020000601707.
9. Arayapisit T., Ngamsom S., Duangthip P., et al. Understanding the mandibular condyle morphology on panoramic images: a cone beam computed tomography comparison study. Cranio 2023; 41(4):354-61. Doi: 10.1080/08869634.2020.1857627.
10. Healy MJR., Goldstein H. An approach to the scaling of categorized attributes. Biometrika 1976; 63(2):219-29. Doi: 10.1093/biomet/63.2.219.
11. Nishisato Shizuhiko. Analysis of Categorical Data: Dual Scaling and its Applications. Toronto: University of Toronto Press; 1980.
12. Van Elslande DC., Russett SJ., Major PW., Flores-Mir C. Mandibular asymmetry diagnosis with panoramic imaging. Am J Orthod and Dentofacial Orthop 2008; 134(2): 183-92. Doi: 10.1016/j.ajodo.2007.07.021.
13. Sonal V., Sandeep P., Kapil G., Christine R. Evaluation of condylar morphology using panoramic radiography. Journal of Advanced Clinical and Research Insights 2016; 3(1):5-8. Doi: 10.15713/ins.jcri.94.
14. Yavan MA., Isman E., Kocahan S. Evaluation of condylar structures on panoramic radiographs in adolescent patients with coeliac disease. Folia Morphol (Warsz) 2019; 78(1):191-4. Doi: 10.5603/FM.a2018.0051.
15. Hegde R., Shigli A., Gawali P., Krishnan A., Jadhav G., Raheja S. Morphological variations of the condylar head among children aged 4-15 years: a panoramic study. J Indian Soc Pedod Prev Dent 2021; 39(4):353–7. Doi: 10.4103/jisppd.jisppd_363_21.
16. Onem Ozbilen E., Turan B., Başal E., Yıldırım G. Evaluation of mandibular condyle shape distribution using digital panoramic images. European Journal of Research in Dentistry 2023; 7(2):89-94. Doi: 10.29228/erd.50.
17. Khanal P., Pranaya K. Study of mandibular condyle morphology using orthopantomogram. JNDA 2020; 20(1):3-7.
18. Tanu LG., Polii H., Lesmana D. Morphological appearance of condylar head in mixed dentition period (evaluated from panoramic radiograph). Preprints 2021. Doi: 10.20944/preprints202101.0121.v1.

EVALUATION OF CLINICOPATHOLOGICAL CHARACTERISTICS IN SINGLE-ORGAN CUTANEOUS SMALL VESSEL VASCULITIS
SINGLE-ORGAN CUTANEOUS SMALL VESSEL VASCULITIS

TEK-ORGAN KUTANÖZ KÜÇÜK DAMAR VASKÜLİTİNİN KLİNİKOPATOLOJİK ÖZELLİKLERİNİN DEĞERLENDİRİLMESİ
TEK-ORGAN KUTANÖZ KÜÇÜK DAMAR VASKÜLİTİ

Erkan DAVARCI[1], Fatma Sule AVSAR[2], Nuket OZKAVRUK ELIYATKIN[*3]

[1]Izmir Katip Celebi University, Izmir Atatürk Training and Research Hospital, Dermatology Department, Izmir, Türkiye. e-mail: drerkandavarci@gmail.com
[2]Izmir Katip Celebi University, Izmir Atatürk Training and Research Hospital, Dermatology Department, Izmir, Türkiye. e-mail: suleafsar@hotmail.com
[*3] Izmir Katip Celebi University, Faculty of Medicine, Izmir Atatürk Training and Research Hospital, Pathology Department, Izmir, Türkiye. e-mail: nuket.ozkavruk.eliyatkin@ikcu.edu.tr

ORCID ID: ED: 0000-0002-7156-0406 **FSA:** 0000-0002-9103-2782 **NOE:** 0000-0002-7784-5699

DOI: 10.52818/cjmr.1582681 **E-ISSN:** 2791-7061

ARTICLE INFO

Article Information

Article Type:
Research Article
Received: 10.11.2024
Accepted: 14.04.2025
Published: 30.04.2025

Keywords:
Single-organ cutaneous small vessel vasculitis,
Clinical features,
Histopathology

ABSTRACT

Objective: Cutaneous vasculitis includes a wide and heterogeneous spectrum of vasculitic syndromes characterized by inflammation of skin blood vessels. When the disease is confined to the skin, the term single-organ cutaneous small vessel vasculitis is used. Data regarding this entity is limited. This study aims to retrospectively evaluate the clinicopathological characteristics of patients who were diagnosed with single-organ cutaneous small vessel vasculitis retrospectively.

Material and Methods: One hundred eight patients were included in the study. Demographic characteristics, clinical features, laboratory findings, etiological factors, treatment modalities, and prognoses of 108 patients were evaluated. Biopsy specimens of patients were re-evaluated histopathologically.

Results: Most frequently acral involvement, and palpable purpura were observed in 82.4% of the patients. Clinical presentation was acute in 80 (74.1%) patients and relapse was seen in 24 (23.1%) patients. Relapse and ulcerative lesions were observed more frequently in chronic patients. The mean age was found to be lower in relapsing patients. Etiology was idiopathic in 75% of the patients. The elevation of CRP was significant in patients with severe fibrinoid necrosis and subcutaneous tissue involvement. Treatment option with topical corticosteroids and nonsteroidal anti-inflammatory drugs (54,3%) was the most common type. The clinical and histopathological features were found to have no effect on relapse, but treatment type was associated with relapse.

Conclusion: There are few studies on single organ cutaneous small vessel vasculitis. Results were similar to the features of the other studies. Further studies in which clinical and histopathological features will be evaluated together are needed.

MAKALE BİLGİLERİ

Makale Bilgisi

Makale Türü:
Araştırma Makalesi
Geliş Tarihi: 10.11.2024
Kabul Tarihi: 14.04.2025
Yayım Tarihi : 30.04.2025

Anahtar Kelimeler:
Tek-organ kutanöz küçük damar vasküliti,
Klinik özellikler,
Histopatoloji

ÖZET

Amaç: Kutanöz vaskülit, deri kan damarlarının enflamasyonu ile karakterize geniş ve heterojen bir vaskülitik sendrom spektrumunu içerir. Hastalık deriyle sınırlı olduğunda, tek organlı kutanöz küçük damar vasküliti terimi kullanılır. Bu antiteye ilişkin veriler sınırlıdır. Bu çalışmada tek organlı kutanöz küçük damar vasküliti tanısı alan hastaların klinikopatolojik özelliklerinin retrospektif olarak değerlendirilmesi amaçlanmıştır.

Gereç ve Yöntemler: Yüz sekiz hasta çalışmaya dahil edildi. Hastaların demografik özellikleri, klinik özellikleri, laboratuvar bulguları, etiyolojik faktörleri, tedavi modaliteleri ve prognozları değerlendirildi. Hastaların biyopsi örnekleri histopatolojik olarak yeniden değerlendirildi.

Bulgular: Hastaların %82,4'ünde akral tutulum mevcuttu. Palpabl purpura (%82,4) en sık görülen deri lezyonuydu. Klinik prezentasyon 80 (%74,1) hastada akut iken, 24 (%23,1) hastada nüks görüldü. Kronik hastalarda nüks ve ülseratif lezyonlar daha sık gözlendi. Nüks eden hastalarda yaş ortalaması daha düşük bulundu. Hastaların %75'inde etiyoloji idiyopatikti. CRP yüksekliği şiddetli fibrinoid nekroz ve subkutan doku tutulumu olan hastalarda anlamlıydı. Topikal kortikosteroidler ve nonsteroid antiinflamatuvar ilaçlarla tedavi seçeneği (%54,3) en yaygın tipti. Klinik ve histopatolojik özelliklerin nüks üzerinde etkisi olmadığı, ancak tedavi tipinin nüks ile ilişkili olduğu bulunmuştur.

Sonuç: Tek organ kutanöz küçük damar vasküliti ile ilgili az sayıda çalışma vardır. Sonuçlar diğer çalışmaların özelliklerine benzerdi. Klinik ve histopatolojik özelliklerin birlikte değerlendirileceği ileri çalışmalara ihtiyaç vardır.

Davarci E., Avsar FS., Ozkavruk Eliyatkın N. Evaluation of Clinicopathological Characteristics in Single-organ Cutaneous Small Vessel Vasculitis. CJMR 2025; 5(1):22-36
Correspondence to: Nuket Ozkavruk Eliyatkin Izmir Katip Celebi University, Faculty of Medicine, Department of Pathology, Izmir, Turkey
Authorship Contributions: Concept: ED, FSA, NOE Design: ED, FSA, NOE Supervision: FSA Resources: ED, FSA, NOE Data Collection and Procesing: ED, FSA, NOE Analysis and Interpretation: ED, FSA Literature Search: ED, FSA, NOE Writing Manuscript: ED, NOE Critical Review: ED, FSA, NOE

Conflict of Interest: The authors report no conflicts of interest.

Ethical Approval: The study was approved by the Ethics Committee of Izmir Ataturk Training and Research Hospital and adhered to the principles of the Declaration of Helsinki (2020GOKAE-0374) on 17 September 2020

Introduction

Cutaneous vasculitis is an inflammatory disease affecting the dermal blood vessel walls. The skin, as the organ primarily involved in vasculitis, facilitates physical examination and safe biopsy, thus allowing accurate identification of inflammatory lesions of the cutaneous vasculature. Cutaneous vasculitis may present clinically as cutaneous component of vasculitis, the cutaneous limited component of systemic vasculitis or the cutaneous predominant expression or single organ vasculitis alone. Multiple and polymorphic vasculitis lesions have a wide spectrum of clinical manifestations depending on the location and size of the blood vessels involved. The type of inflammatory infiltration is also a key finding in the diagnosis of cutaneous vasculitis (1).

In 2012, the International Chapel Hill Consensus Conference (CHCC) defined single-organ vasculitis affecting arteries or veins of any size in only a single organ without systemic involvement. If the vasculitis is limited to the skin, the term single-organ cutaneous small vessel vasculitis (SoCSVV) was adopted. The presence of characteristic leukocytoclastic vasculitis (LCV) on biopsy and vasculitis confined to the skin were stated as the diagnostic criteria for (SoCSVV) (2).

There are limited number of studies on SoCSVV in the literature (3-5). Although the disease is a self-limiting condition with good clinical outcomes, significantly higher relapse rates and challenges in its treatment may be experienced due to complications encountered during daily clinical practice (6). In our study, we aimed to screen and clinicopathologically evaluate patients diagnosed with cutaneous vasculitis in terms of additional systemic involvement and to investigate clinical and histopathologic features, etiologic factors, treatment modalities and prognosis of the patients who fulfilled the diagnostic criteria of SoCSVV.

Materials and Methods

Patient population

In this study, patients diagnosed with vasculitis based on histopathological examination of their skin biopsy specimens in the Dermatology Clinic of IKCU Atatürk Training and Research Hospital between 2006 and 2020 were analyzed. Clinical and laboratory data of the patients were retrieved retrospectively from patient files and electronic medical records.

Skin biopsy specimens of these patients stored in the pathology archive were re-evaluated by a pathologist, and patients diagnosed with LCV were evaluated once more in terms of clinical features and systemic involvement elaborated below. LCV was defined as neutrophil infiltration in the vessel wall, swelling of endothelial cells, erythrocyte extravasation and fibrinoid necrosis and nuclear dust (dust), which are characteristic findings in skin biopsy (7). In 2012, patients in the group defined as SoCSVV without other organ involvement, which was accepted in CHCC, constituted the population of the study.

Clinical and laboratory definitions

A total of 108 patients diagnosed with SoCSVV were evaluated in terms of age, gender, type of skin lesions (palpable purpura, ulcerative lesion, palpable purpura+non-palpable purpura, palpable purpura+vesicle/bulla), area involved (acral, generalized), clinical presentation (acute, chronic), etiological factors (idiopathic, drug, infection, drug+infection), treatment modalities and prognosis (complete remission, relapse). Single episodes lasting less than three months were considered acute, prolonged disease course lasting longer than three

months or recurrent episodes at least twice in a period exceeding three months were considered chronic SoCSVV. Relapses were defined as recurrence of vasculitis symptoms following a remission period of more than one month.

Complete blood counts, results of liver, kidney function, fecal occult blood tests, hepatitis B, hepatitis C and HIV serologies, levels of antinuclear antibody (ANA), serum complement, anti-neutrophil cytoplasmic antibodes (p-ANCA, and c-ANCA), rheumatoid factor (RF), and chest X-ray findings of the patients were re-evaluated in terms of the presence of systemic involvement. Inflammation markers of patients diagnosed with SoCSVV as C-reactive protein (CRP) and erythrocyte sedimentation rate (ESR) were also evaluated.

Skin biopsy specimens were evaluated histopathologically for the presence of neutrophilic infiltration in the vessel wall, swelling of endothelial cells, erythrocyte extravasation and fibrinoid necrosis (fibrin deposition in the vessel wall), nuclear dust, leukocytoclasia, perivascular cell infiltration, ulcer-necrosis, granuloma, endothelial change and subcutaneous tissue involvement which are characteristic diagnostic features of LCV (7).

Statistical analysis

Statistical analysis of the data was performed using SPSS 22.0 program. Chi-square test was used to reveal the differences between nominal and ordinal variables, Mann-Whitney U and Wilcoxon tests were used to examine the differences between independent variables, and Student-t test was used to evaluate numerical variables with normal distribution characteristics. Logistic regression test was used for prognostic and predictive factors. P values of 0.05 and below were considered statistically significant.

Results

A total of 108 patients with a mean age of 52.21±19.98 years including 58 (53.7%) female, and 50 (46.3%) male cases (female/male: 1.16) among 728 patients diagnosed with vasculitis based on their clinical features and histopathological examination findings of their skin biopsy specimens archived between 2006 and 2020 and re-evaluated according to International CHCC criteria, received the diagnosis of SoCSVV. The flow chart of the study is shown in Figure 1.

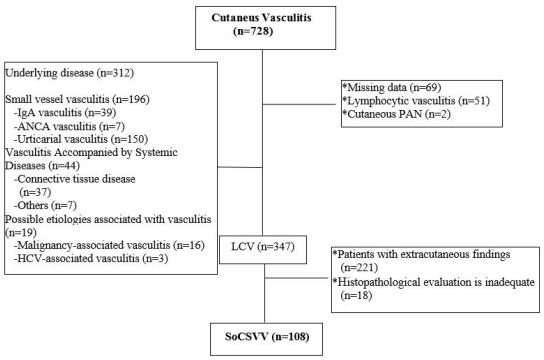

Figure 1. *The flow chart of the study.*

The distribution of the patients in terms of involved area, skin lesions, clinical presentation and prognosis is shown in Table 1.

Table 1. *Distribution of patients with SoCSVV in terms of affected area, skin lesions, clinical presentation and prognosis.*

	n	%
Affected area	108	100
Acral	89	82,4
Generalized	19	17,6
Skin lesions	108	100
Palpable purpura	89	82,4
Ulcerative lesion	10	9,3
Palpable purpura + non-palpable purpura	5	4,6
Palpable purpura + vesicle/bulla	4	3,7
Clinical presentation	108	100
Acute	80	74,1
Chronic	28	25,9
Prognosis	104	100
Relapse	24	23,1
Complete remission	80	76,9

Biopsy specimens of 108 patients diagnosed with SoCSSV were evaluated for histopathologic features of LCV such as neutrophils in the vessel wall, fibrinoid necrosis (Figure 2), nuclear dust (Figure 3), erythrocyte extravasation (Figure 4) and severity of these features. In addition, perivascular cell infiltration (Figure 5), ulcer-necrosis, granuloma, endothelial change (Figure 2), and involvement of subcutaneous tissue (Figure 6) were included in the histopathologic evaluation. Granuloma was not detected in any patient.

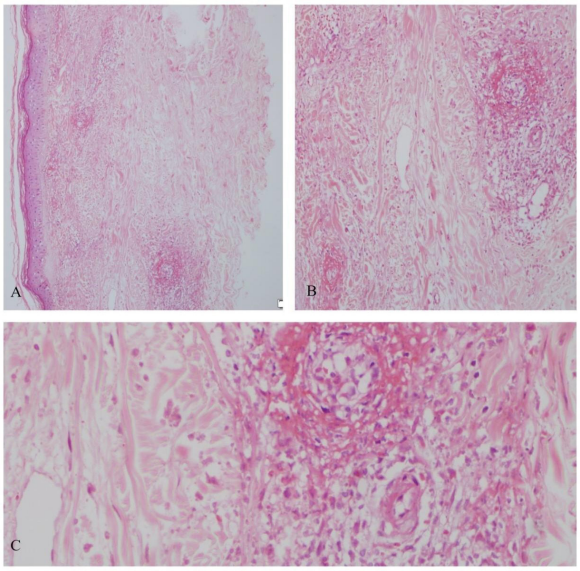

Figure 2. *(A) Fibrinoid necrosis (Hematoxylin-Eosin x 100), (B) Fibrinoid necrosis (Hematoxylin-Eosin x 200), (C) Fibrinoid necrosis and endothelial shedding and swelling (Hematoxylin-Eosin x 400).*

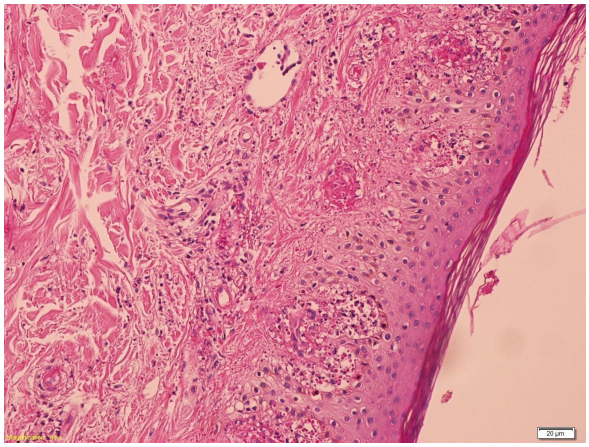

Figure 3. *Fibrinoid necrosis and nuclear dust (Hematoxylin-Eosin x 200).*

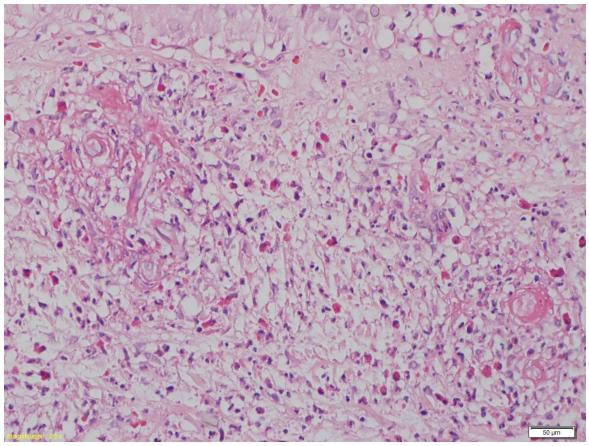

Figure 4. *Erythrocyte extravasation, neutrophil+eosinophil infiltration and fibrinoid necrosis (Hematoxylin-Eosin x 400).*

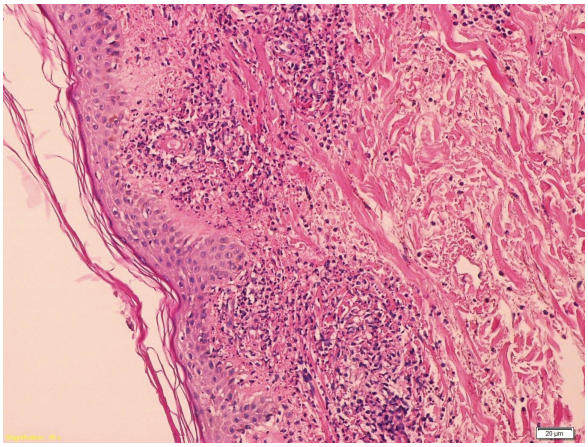

Figure 5. *Perivascular cell infiltration and nuclear dust (Hematoxylin-Eosin x 200).*

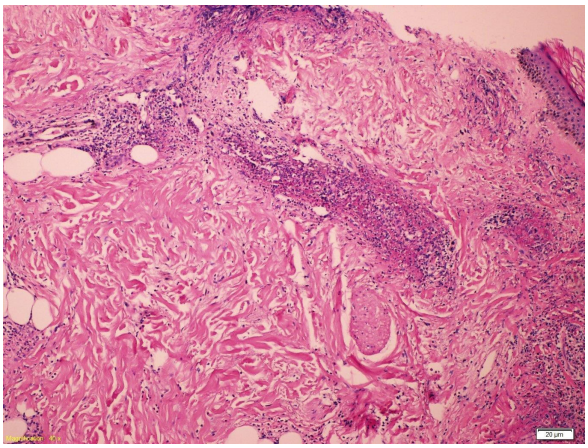

Figure 6. *Polymorphonuclear cell infiltration and fibrinoid necrosis including subcutaneous tissue involvement (Hematoxylin-Eosin x 100).*

The comparison of clinical and histopathologic features according to acute and chronic presentation of vasculitis in 108 patients with SoCSSV is shown in table 2. Clinical characteristics (gender, area involved, type of skin lesions, etiologic factors, prognosis) and histopathologic features (neutrophil infiltration in the vessel wall, fibrinoid necrosis, nuclear dust, erythrocyte extravasation, perivascular cell infiltration, endothelial change, level of involvement) in terms of acute and chronic presentation of vasculitis, a statistically significant difference was found between acute and chronic cases in terms of type of skin lesions and prognosis ($p<0.05$). While ulcerative lesions were less common in acute cases compared to chronic cases, complete remission rates were significantly higher than chronic cases. No statistically significant difference was found between the other groups compared.

Table 2. *Comparison of clinical and histopathological features in patients with SoCSSV according to acute and chronic presentation of vasculitis.*

		Clinical presentation				χ2	p
		Acute		Chronic			
		n	%	n	%		
Gender	Female	45	56,3	13	46,4	0,805	0,370
	Male	35	43,8	15	53,6		
Affected area	Acral	65	81,3	24	85,7	0,285	0,775
	Generalized	15	18,8	4	14,3		
Skin lesions	Palpable purpura	69	86,3	20	71,4		
	Ulcerative lesion	3	3,8	7	25,0		
	Palpable purpura + Non-palpable purpura	4	5,0	1	3,6	10,021	0,009
	Palpable purpura + vesicle/bulla	4	5,0	-	-		
Palpable purpura	No	11	13,8	8	28,6	3,143	0,089
	Yes	69	86,3	20	71,4		
Ulcerative lesion	No	77	96,3	21	75,0	11,147	0,003
	Yes	3	3,8	7	25,0		
Palpable purpura + non-palpable purpura	No	76	95,0	27	96,4	0,096	1,000
	Yes	4	5,0	1	3,6		
Palpable purpura + vesicle/bulla	No	76	95,0	28	100,0	1,454	0,571
	Yes	4	5,0	-	-		
Etiology	Idiopathic	57	71,3	24	85,7		
	Drug	14	17,5	2	7,1	2,440	0,568
	Infection	4	5,0	1	3,6		
	Drug&infection	5	6,3	1	3,6		
Prognosis	Complete remission	76	97,4	4	15,4	73,956	<0,001
	Relapse	2	2,6	22	84,6		
Neutrophils in the vascular wall	Mild-Moderate	40	50,0	12	42,9	0,424	0,515
	Severe	40	50,0	16	57,1		
Fibrinoid necrosis	Mild-Moderate	40	50,0	12	42,9	0,424	0,515
	Severe	40	50,0	16	57,1		
Nuclear dust	Mild-Moderate	32	40,0	13	46,4	0,353	0,553
	Severe	48	60,0	15	53,6		
Erythrocyte extravasation	Mild-Moderate	48	60,0	14	50,0	0,848	0,357
	Severe	32	40,0	14	50,0		
Perivascular cell infiltration	Neutrophil+less eosinophil or neutrophil+eosinophil	18	22,5	6	21,4		
	Neutrophil or eosinophil or lymphocyte or neutrophil+lymphocyte or mixt	62	77,5	22	78,6	0,014	0,907
Endothelial change	No	11	13,8	4	14,3		
	Shedding	7	8,8	2	7,1		
	Swelling	34	42,5	14	50,0	3,854	0,399
	Shedding+Swelling	27	33,8	6	21,4		
	Uncertain	1	1,3	2	7,1		
Involvement of the subcutaneous tissue	No	29	47,5	10	47,6	<0,001	0,995
	Yes	32	52,5	11	52,4		

Pearson Chi-Square, Fisher's Exact test

The comparison of clinical features, treatment modalities and histopathological features in 108 patients with SoCSSV in terms of CRP elevation is shown in table 3. When the mean age distribution of the patients evaluated as SoCSVV was statistically compared in terms of gender, clinical presentation, area of involvement, type of skin lesions and etiologic factors, the age of patients with complete remission according to prognosis was significantly higher than the age of patients with relapse ($p<0.05$). No statistically significant difference was found between the other groups compared. CRP elevation among inflammatory markers, clinical features of SoCSVV (gender, clinical presentation, area involved, type of skin lesions, etiologic factors, prognosis), preferred treatment modalities and histopathologic features (neutrophil infiltration in the vessel wall, fibrinoid necrosis, nuclear dust, erythrocyte extravasation, perivascular cell infiltration, endothelial change, involvement level), there was a statistically significant difference between treatment modalities and histopathologic features of fibrinoid necrosis and involvement level ($p<0.05$). When treatment modalities were compared in pairs, CRP elevation was statistically significant in colchicine and systemic corticosteroid treatment, topical corticosteroid and NSAID treatment and topical corticosteroid and systemic corticosteroid treatment. In patients with histopathologically severe fibrinoid necrosis, there was a statistically significant CRP elevation compared to those with moderate to mild fibrinoid necrosis. CRP elevation was statistically significant in patients with subcutaneous tissue involvement compared to patients without subcutaneous tissue involvement. No statistically significant difference was found between the other groups compared (Table 3).

Table 3. *Comparison of clinical features, treatment modalities and histopathological features in patients with SoCSSV in terms of CRP elevation.*

		CRP				χ^2	p
		Normal		High			
		n	%		%		
Gender	Female	17	53,1	36	54,5	0,018	0,895
	Male	15	46,9	30	45,5		
Clinical presentation	Acute	22	68,8	51	77,3	0,824	0,364
	Kronik	10	31,3	15	22,7		
Affected area	Akral	29	90,6	54	81,8	1,289	0,256
	Generalize	3	9,4	12	18,2		
Skin lesions	Palpable purpura	30	93,8	55	83,3		
	Ulcerative Lesion	1	3,1	6	9,1	3,205	0,355
	Palpable purpura + Non-palpable purpura	1	3,1	1	1,5		
	Palpable purpura + Vesicle/bulla	0	0,0	4	6,1		
Etiology	Idiopathic	24	75,0	50	75,8		
	Drug	4	12,5	9	13,6	0,456	1,000
	Infection	2	6,3	3	4,5		
	Drug&Infection	2	6,3	4	6,1		
Treatment	Topical Corticosteroid + NSAID	17	54,8	38	57,6		
	Topical Corticosteroid + Colchicine	3	9,7	3	4,5		
	Topical Corticosteroid + Systemic Corticosteroid	5	16,1	23	34,8	9,732	0,013
	Colchicine + Systemic Corticosteroid	6	19,4	2	3,0		

Paired Matching in Treatment	Topical Corticosteroid + NSAID *vs* Topical Corticosteroid +Colchicine						0,384
	Topical Corticosteroid+NSAID *vs* Topical Corticosteroid+Systemic Corticosteroid						0,294
	Colchicine+Systemic Corticosteroid						0,043
	Topical Corticosteroid + Colchicine vs Topical Corticosteroid + Systemic Corticosteroid						0,126
	Topical Corticosteroid + Colchicine vs Colchicine+Systemic Corticosteroid						0,0580
	Topical Corticosteroid + Systemic Corticosteroid vs Colchicine + Systemic Corticosteroid						0,005
Prognosis	Complete remission	22	71,0	52	81,3	1,282	0,257
	Relapse	9	29,0	12	18,8		
Neutrophils in the vascular wall	Mild-Moderate	13	40,6	31	47,0	0,351	0,554
	Severe	19	59,4	35	53,0		
Fibrinoid necrosis	Mild-Moderate	20	62,5	26	39,4	4,620	0,032
	Severe	12	37,5	40	60,6		
Nuclear dust	Mild-Moderate	12	37,5	27	40,9	0,105	0,746
	Severe	20	62,5	39	59,1		
Erythrocyte extravasation	Mild-Moderate	18	56,3	36	54,5	0,025	0,874
	Severe	14	43,8	30	45,5		
Perivascular cell infiltration	Neutrophil+less osinophil or neutrophil+ eosinophil	10	31,3	13	19,7	1,601	0,206
	Neutrophil or eosinophil or lymphocyte or neutrophil+lymphocyte or mixt	22	68,8	53	80,3		
Endotelial change	No	4	12,5	8	12,1		
	Shedding	1	3,1	6	9,1		
	Swelling	17	53,1	29	43,9	1,599	0,866
	Shedding+Swelling	9	28,1	21	31,8		
	Uncertain	1	3,1	2	3		
Involvement of the subcutaneous tissue	No	15	62,5	18	36,7	4,317	0,038
	Yes	9	37,5	31	63,3		

Pearson Chi-Square, Fisher's Exact test

For direct immunofluorescence (DIF) examination, 38 (35.1%) of one hundred and eight patients were sampled and only 5 (13.1%) of them were positive. Two (40%) patients had isolated IgG positivity, one (20%) patient had isolated C3 positivity, and two (40%) patients had IgG and C3 positivity.

Since cutaneous biopsy specimens of twenty-six (24.08%) patients did not include subcutaneous tissue, when the relationship between subcutaneous tissue involvement and area of involvement, type of skin lesions, etiologic factors and prognosis was investigated in 82 (75.92%) SoCSVV patients, a statistically significant difference was found in terms of the type of skin lesions ($p<0.05$). Histopathologically, the frequency of ulcerative lesions in patients with subcutaneous tissue involvement was statistically significantly higher than in patients without subcutaneous tissue involvement, while the frequency of palpable purpura in patients without subcutaneous tissue involvement was statistically significantly higher than in patients with subcutaneous tissue involvement. No statistically significant difference was found between the other groups compared (Table 4).

Table 4. *Relationship between subcutaneous tissue involvement and the area of involvement, type of skin lesions, etiological factors and prognosis in patients with SoCSVV.*

		Involvement of the subcutaneous tissue				X^2	p
		No		Yes			
		n	%	n	%		
Affected area	Acral	30	76,9	38	88,4	1,893	0,169
	Generalized	9	23,1	5	11,6		
Skin lesion	Palpable purpura	36	92,3	32	74,4		
	Ulcerative lesion	-	-	8	18,6		
	Palpable purpura + non- palpable purpura	3	7,7	1	2,3	11,169	0,003
	Palpable purpura + vesicle/bulla	-	-	2	4,7		
Palpable purpura	No	3	7,7	11	25,6	4,623	0,032
	Yes	36	92,3	32	74,4		
Ulcerative lesion	No	39	100,0	35	81,4	8,040	0,006
	Yes	-	-	8	18,6		
Palpable purpura + non-palpable purpura	No	36	92,3	42	97,7	1,269	0,342
	Yes	3	7,7	1	2,3		
Palpable purpura + vesicle/bulla	No	39	100,0	41	95,3	1,859	0,495
	Yes	-	-	2	4,7		
Etiology	Idiopathic	26	66,7	35	81,4		
	Drug	10	25,6	3	7,0	5,497	0,126
	Infection	2	5,1	3	7,0		
	Drug&infection	1	2,6	2	4,7		
Prognosis	Complete remission	27	73,0	33	80,5	0,619	0,432
	Relapse	10	27,0	8	19,5		

Pearson Chi-Square, Fisher's Exact test

When the relationship between the type of skin lesions in patients with SoCSVV and gender, etiologic factors, treatment options and prognosis was investigated, no statistically significant difference was found between the groups. One hundred and eight patients with SoCSVV were treated in 105 patients (97.2%). When the treatment modalities of the treated patients were compared in terms of area of involvement, type of skin lesions, etiologic factors and clinical presentation of vasculitis, a statistically significant difference was found between the treatment modalities in terms of clinical presentation ($p<0.05$). The rate of chronic presentation was significantly higher in patients given topical corticosteroids and NSAIDs than in patients given topical corticosteroids and colchicine, topical corticosteroids and systemic corticosteroids, and colchicine and systemic corticosteroids. No statistically significant difference was found between the other groups compared (Table 5). When gender, area of involvement, type of skin lesions, etiologic factors, ESR elevation, CRP elevation, treatment modalities and histopathologic features that may affect prognosis in patients with SoCSVV were evaluated by single logistic regression analysis, topical corticosteroids and NSAIDs, topical corticosteroids and colchicine, and colchicine and systemic corticosteroids were found to be statistically significant for relapse ($p<0.05$).

Table 5. *Comparison of treatment modalities in patients with SoCSVV in terms of area of involvement, type of skin lesions, etiological factors and clinical presentation.*

		Treatment								X^2	p
		Topical Corticosteroid + NSAID		Topical Corticosteroid + Colchicine		Topical Corticosteroid +Systemic Corticosteroid		Colchicine +Systemic Corticosteroid			
		n	%	n	%	n	%	n	%		
Affected area	Acral	50	87,7	6	85,7	25	75,8	6	75	2,856	0,390
	Generalized	7	12,3	1	14,3	8	24,2	2	25		
Skin lesions	Palpable purpura	49	86	4	57,1	26	78,8	8	100		
	Ulcerative lesion	2	3,5	2	28,6	6	18,2	-	-		
	Palpable purpura + non-palpable purpura	2	3,5	1	14,3	1	3	-	-	13,214	0,071
	Palpable purpura + vesicle/bulla	4	7	-	-	-	-	-	-		
Etiology	Idiopathic	39	68,4	6	85,7	25	75,8	8	100		
	Drug	10	17,5	1	14,3	5	15,2	-	-	3,694	0,937
	Infection	3	5,3	-	-	2	6,1	-	-		
	Drug&infection	5	8,8	-	-	1	3	-	-		
Clinical presentation of vasculitis	Acute	50	87,7	3	42,9	23	69,7	3	37,5	14,702	0,001
	Chronic	7	12,3	4	57,1	10	30,3	5	62,5		
	Acute	50	87,7	3	42,9					0,014	
	Chronic	7	12,3	4	57,1						
	Acute	50	87,7	10		23	69,7			0,035	
	Chronic	7	12,3			30,3					
	Acute	50	87,7			5	62,5	3	37,5	0,004	
	Chronic	7	12,3								
	Acute	4		3	42,9	23	69,7			0,214	
	Chronic			57,1	10	30,3					
	Acute	4		3	42,9	5	62,5	3	37,5	1,000	
	Chronic			57,1							
	Acute			10	30,3	23	69,7	3	37,5	0,117	
	Chronic					5	62,5				

Fisher's exact test

Discussion

Defined in the 2012 CHCC, SoCSVV is considered a vasculitis affecting the skin without involvement of vessels in any other organ. Therefore, few patients with LCV may fulfill the SoCSVV criteria (2). SoCSVV usually presents with a good clinical picture and the prognosis is mild. Although less frequent, the fact that the disease may progress with relapses may lead to increased costs and patient concerns (6).

Since SoCSVV has been defined relatively recently, epidemiologic and clinical data are limited. In our retrospective study, the mean age of patients with SoCSVV was 52.21±19.98 years and a slight female predominance was found. In studies conducted with patients with SoCSVV, the mean age was found to be 66.9, 50 and 56 years, with a slight female predominance in only one study (6, 8-9). In a study on LCV including 75 patients in Türkiye, the mean age was found to be 43.5 years (10). In a more

comprehensive review, the mean age in cutaneous vasculitis was reported to be 47 years (11). In a study in which patients with SoCSVV were compared with the LCV patient group, the mean age of the patient group with SoCSVV was found to be higher (9). When evaluated together with the clinical characteristics, the mean age of the patients who were found to have complete remission in our study was higher than the patients who showed relapse and it was thought that the possibility of relapse was higher in younger patients with SoCSVV.

When the distribution of skin lesions was examined, nearly all patients had lower extremity involvement. Consistent with our study, Bouiller et al. reported acral involvement in 79.3% of patients with SoCSVV (9), and Pastuszczak et al. reported acral involvement in 83.3% of patients with SoCSVV (6). The most common clinical manifestation of LCV is palpable purpura, which occurs mostly on the feet and lower extremities. Lesions can also occur on the forearms and hands. may be observed, but it is not frequently observed in the upper part of the trunk. Similar to previous studies, palpable purpura was observed in 90.7% of patients in our study, ulcerative lesions were present in 9.3%. In other studies conducted with patients with SoCSVV, ulcer rates were found to be 17.2% and 16.7%, which are slightly higher than our study (6, 9).

According to the anamnesis at the time of presentation, 80 (74.1%) of the patients in our study had an acute course and 28 (25.9%) had a chronic course. In the few studies conducted with SoCSVV, there was no information on whether the patients presented with acute or chronic symptoms. In the study by Bouiller et al, it was reported that skin lesions persisted for one month or more in 27.6% of twenty-nine SoCSVV patients (9). In a study involving 82 patients with LCV, it was reported that 56.09% of the patients presented with acute clinic (12). In another study on cutaneous vasculitis, chronic presentation was found to be approximately 20% (11).

Known etiologic causes of cutaneous vasculitis include infections, connective connective tissue diseases, drug reactions and malignancies (13). In our study, 75% of the patients with SoCSVV were evaluated as idiopathic. This rate was found to be 45.8% and 46.7% in two other studies conducted with patients with SoCSVV. In the same two studies, drug etiology was reported as 16.7% and 25%, respectively (6, 8). In our study, the rate of drugs among etiologic factors was 14.8%. The high rate of idiopathic etiology in our study may be explained by the fact that the study was retrospective and did not have sufficient anamnesis data. In a review including studies on CSVV, the rate of patients with drugs in the etiology was reported as 10-15%, similar to our study (14).

Among the 108 patients with SoCSVV included in our study, 105 were treated. In a study involving sixty SoCSVV patients, it was reported that 33.3% of the patients received treatment and 13.3% of these patients received NSAIDs, 15% received systemic corticosteroids, 3.3% received antihistamines and 1.7% received colchicine (8). In a study including 29 patients with SoCSVV, it was reported that only 17.2% of the patients received a specific treatment and this treatment was prednisone treatment (9). In another study involving twenty-four patients with SoCSVV, it was reported that 70.8% of the patients received treatment, 37.5% of all patients received systemic corticosteroid treatment and 33.3% received systemic antibiotic treatment (6). Although there is not enough data for treatment recommendations for SoCSVV, it has been reported that systemic treatment is not needed for LCV unless there are hemorrhagic bullae

suggestive of necrosis or ulceration or systemic involvement (15). However, the fact that systemic treatment was given to all but three of the patients included in our study shows that conservative treatment approach is not preferred in cases where vasculitis is limited to the skin. It is noteworthy that systemic treatment was given to all those for whom drugs were considered in the etiology.

Elevated CRP was found in 90.7% of patients with inflammation and tissue damage, and elevated ESR, which is used to determine inflammatory activity, was investigated in 91.6% of patients and found to be elevated in 67.3% and 61.6%, respectively. In a study conducted with patients with SoCSVV, CRP elevation was found in 78.6% of patients and ESR elevation was found in 86.4% of patients, and these rates were slightly higher compared to our study (9). In another study including patients with SoCSVV, it was reported that one of the most common laboratory findings was elevated ESR, but the rate was not specified (8). In a study investigating patients with LCV, CRP values of 196 patients were examined and CRP values were found to be elevated in 70.91% of the patients (16). In a retrospective study of 275 patients with cutaneous vasculitis, it was reported that 49.1% had elevated CRP and 72.9% had elevated ESR (17).

When evaluated together with histopathologic features, CRP elevation was found to be significant in cases with severe fibrinoid necrosis and in cases with subcutaneous tissue involvement. Colchicine and systemic corticosteroid treatment was preferred in patients with high CRP values. However, no correlation was found between clinical and histopathologic features and ESR elevation in our study. There is insufficient data on the relationship between inflammatory markers and histopathologic features of vasculitis. In a study one hundred and seventy patients with cutaneous vasculitis, no significant relationship was found between ESR elevation and clinicopathologic features (17).

In our study, involvement in subcutaneous tissue was observed in about half of the patients with subcutaneous tissue in the biopsy samples of patients with SoCSVV. Histopathologic features were not mentioned in detail in the limited number of studies conducted with patients with SoCSVV, and only one study reported involvement in subcutaneous tissue in 53% of patients, which is compatible with our study (6,8-9). Ulcer-necrosis was observed in 12.03% of the patients. Granuloma formation was not observed in any patient. In a study including 56 patients in which cutaneous vasculitis was evaluated, it was reported that 75% of patients had LCV, 17.8% had lymphocytic vasculitis, 1.78% had eosinophilic vasculitis and 1.78% had granulomatous vasculitis. As a result of this evaluation, inflammatory cell infiltration was observed in all cases, followed by leukocytoclasia (nuclear dust) in 53.5%, endothelial cell swelling in 50%, and dermal edema in 46.4%. Fibrin deposition was found in only 16% of the patients (19). In another study involving fifty-three patients with cutaneous vasculitis, leukocytoclasia (nuclear dust) was reported in 84.9%, fibrinoid necrosis in 88.6%, erythrocyte extravasation in 90.5% and dermal edema in 84.9% (20).

In our study, it was observed that DIF examination could be performed in only a minority of patients. Bouiller et al. reported that samples were taken for DIF in 26 of 29 SoCSVV patients (89.65%) and DIF findings were positive in 69% of these patients (9). In our study, the relationship between clinical features and DIF findings could not be evaluated due to both the low rate of DIF examination in patients and the low rate of positivity in the analyzed samples.

When we evaluated patients with SoCSVV as acute and chronic, we observed that the frequency of ulcerative lesions was low and the frequency of complete remission was high in acute cases. In a study conducted by Tai et al. with 93 cutaneous LCV patients, it was reported that the incidence of ulcerative lesions was higher in chronic cases, which is consistent with our study (21). However, in a retrospective study by Selvarajah et al. with 275 patients with cutaneous vasculitis, it was reported that there was no difference between acute and chronic cases in terms of age and ulcer (17).

The factor affecting the treatment selection in patients with SoCSVV was the predominance of topical corticosteroid and NSAID combination use in patients presenting with acute presentation. In a similar study, 37.5% of the patients were treated with systemic steroids. When these patients were compared with those treated conservatively, significant leukocytosis and CRP elevation were found in the group treated with systemic steroids. The same study reported that there was no significant difference between the groups treated with and without systemic steroids in terms of the type of skin lesions, the area involved, and other clinical and laboratory results (6). There are few studies on the factors determining relapse in patients with LCV (12, 22). While relapse was seen in 23.1% of our study, no significant relationship was found with other characteristics other than treatment choices as a result of the analysis performed for the clinical and histopathological features thought to be effective in the occurrence of relapse. The frequency of relapse in patients using topical corticosteroids and NSAIDs, topical corticosteroids and colchicine, and colchicine and systemic steroids was significant compared to patients using the other treatment option, topical corticosteroids and systemic corticosteroids. It can be suggested that the combined use of topical and systemic corticosteroids may be effective in preventing relapse in SoCSVV. In a study of 29 SoCSVV patients, it was suggested that no relapse was observed in any SoCSVV patient, on the contrary, SoCSVV itself was a protective factor (135). In the study conducted by Pastuszczak et al., relapse was observed in 25% of 24 SoCSVV patients, no relationship was found between relapse and treatment modalities, but it was reported that patients with more affected body areas in the first attack had a higher risk of relapse (6).

In the study conducted by Loricera et al., it was stated that relapse was observed in 8.3% of 60 SoCSVV patients, and the factors related to relapse were not investigated (8).

Conclusion

In conclusion, although it is suggested that SoCSVV, defined according to the 2012 CHCC criteria, is a benign form of vasculitis, there is limited data on this yet. When the results of this study, in which we investigated the clinicopathological features of SoCSVV, are supported by larger patient groups and prospective studies, this relatively newly defined vasculitis will be better understood.

Limitations

The strength of our study is the relatively high number of patients and the re-evaluation of cutaneous vasculitis biopsy samples by the same pathologist. Its retrospective nature is a limitation. On the other hand, DIF evaluation could not be evaluated in all patients.

References

1.Frumholtz L., Laurent-Roussel S., Lipsker D., Terrier B. Cutaneous vasculitis: review on diagnosis and clinicopathologic correlations. Clin Rev Allergy Immunol 2021; 61(2):181-93. Doi: 10.1007/s12016-020-08788-4.

2.Jennette JC., Falk RJ., Bacon PA., et al. 2012 revised International Chapel Hill Consensus Conference Nomenclature of Vasculitides. Arthritis Rheum 2013; 65(1):1-11. Doi: 10.1002/art.37715.

3.Bodakçi E. Clinical study on single-organ cutaneous small vessels vasculitis: a retrospective observational study. Eur Rev Med Pharmacol Sci 2024; 28(2):534-41. Doi: 10.26355/eurrev_202401_35051.

4.Morita TCAB., Criado PR., Criado RFJ., Trés GFS., Sotto MN. Update on vasculitis: overview and relevant dermatological aspects for the clinical and histopathological diagnosis - Part II. An Bras Dermatol 2020; 95(4):493-507. Doi: 10.1016/j.abd.2020.04.004.

5.Gambichler T., Ardabili L., Domin B., Susok L., Rached NA. Predictors of disease severity, length of hospitalization, and recurrence in inpatients with single-organ cutaneous small vessel vasculitis. Eur J Dermatol 2024; 34(4):378-83. Doi: 10.1684/ejd.2024.4723.

6.Pastuszczak M., Celińska-Löwenhoff M., Sułowicz J., Wojas-Pelc A., Musiał J. Clinical study on single-organ cutaneous small vessels vasculitis (SoCSVV). Medicine (Baltimore) 2017; 96(12):e6376. Doi: 10.1097/MD.0000000000006376.

7.Sunderkötter CH., Zelger B., Chen KR., et al. Nomenclature of Cutaneous Vasculitis: Dermatologic Addendum to the 2012 Revised International Chapel Hill Consensus Conference Nomenclature of Vasculitides. Arthritis Rheumatol 2018; 70(2):171-84. Doi: 10.1002/art.40375.

8.Loricera J., Blanco R., Ortiz-Sanjuán F., et al. Single-organ cutaneous small-vessel vasculitis according to the 2012 revised International Chapel Hill Consensus Conference Nomenclature of Vasculitides: a study of 60 patients from a series of 766 cutaneous vasculitis cases. Rheumatology (Oxford) 2015; 54(1):77-82. Doi: 10.1093/rheumatology/keu295.

9.Bouiller K., Audia S., Devilliers H., et al. Etiologies and prognostic factors of leukocytoclastic vasculitis with skin involvement: A retrospective study in 112 patients. Medicine (Baltimore) 2016; 95(28):e4238. Doi: 10.1097/MD.0000000000004238.

10.Cakiter AU., Kucuk OS., Ozkaya DB., Topukcu B., Onsun N. Demographic characteristics, aetiology, and assessment of treatment options in leukocytoclastic vasculitis. Postepy Dermatol Alergol 2017; 34(2):104-9. Doi: 10.5114/ada.2017.67071.

11.Carlson JA., Ng BT., Chen KR. Cutaneous vasculitis update: diagnostic criteria, classification, epidemiology, etiology, pathogenesis, evaluation and prognosis. Am J Dermatopathol 2005; 27(6):504-28. Doi: 10.1097/01.dad.0000181109.54532.c5.

12.Ekenstam Eaf., Callen JP. Cutaneous leukocytoclastic vasculitis. Clinical and laboratory features of 82 patients seen in private practice. Arch Dermatol 1984; 120(4):484-9. Doi: 10.1001/archderm.120.4.484.

13.Morita TCAB., Trés GFS., Criado RFJ., Sotto MN., Criado PR. Update on vasculitis: an overview and dermatological clues for clinical and histopathological diagnosis - part I. An Bras Dermatol 2020; 95(3):355-71. Doi: 10.1016/j.abd.2020.01.003.

14.Shavit E., Alavi A., Sibbald RG. Vasculitis-what do we have to know? A review of literature. Int J Low Extrem Wounds 2018; 17(4):218-26. Doi: 10.1177/1534734618804982.

15.Cupps TR., Springer RM., Fauci AS. Chronic, recurrent small-vessel cutaneous vasculitis. Clinical experience in 13 patients. JAMA 1982; 247(14):1994-8. PMID: 7062504.

16.Takatu CM., Heringer APR., Aoki V., et al. Clinicopathologic correlation of 282 leukocytoclastic vasculitis cases in a tertiary hospital: a focus on direct immunofluorescence findings at the blood vessel wall. Immunol Res 2017; 65(1):395-401. Doi: 10.1007/s12026-016-8850-6.

17.Latha S., Choon SE., Tey KE., Chee YN. Clinical features and prognostic factors of cutaneous vasculitis among dermatology patients in Johor Bahru, Malaysia. Med J Malaysia 2017; 72(6):345-9. PMID: 29308771.

18.Jennette JC., Falk RJ., Andrassy K., et al. Nomenclature of systemic vasculitides. Proposal of an international consensus conference. Arthritis Rheum 1994; 37(2):187-92. Doi: 10.1002/art.1780370206.

19.Swamy SM., Bhat RM RB. Cutaneous vasculitis : An etiological and clinicopathological study. International Journal of Scientific and Research Publications 2015; 5(9):1-6.

20.Khetan P., Sethuraman G., Khaitan BK, et al. An aetiological & clinicopathological study on cutaneous vasculitis. Indian J Med Res

2012; 135(1):107-13. Doi: 10.4103/0971-5916.93432.

21. Tai YJ., Chong AH., Williams RA., Cumming S., Kelly RI. Retrospective analysis of adult patients with cutaneous leukocytoclastic vasculitis. Australas J Dermatol 2006; 47(2):92-6. Doi: 10.1111/j.1440-0960.2006.00239.x.

22. Sais G., Vidaller A., Jucglà A., Servitje O., Condom E., Peyri J. Prognostic factors in leukocytoclastic vasculitis: a clinicopathologic study of 160 patients. Arch Dermatol 1998; 134(3):309-15. Doi: 10.1001/archderm.134.3.309.

A RARE ENTITY: TWO CASES OF OPTIC NERVE GLIOMA IN ADULTS
OPTIC NERVE GLIOMA IN ADULTS

NADİR BİR DURUM: YETİŞKİNLERDE 2 OPTİK SİNİR GLİOMU OLGUSU
YETİŞKİNLERDE OPTİK SİNİR GLİOMU

Kerem KURT*[1], Nuket OZKAVRUK ELIYATKIN[2], Seyda KARADENIZ UGURLU[3]

[1]Department of Pathology, Izmir Katip Celebi University Ataturk Training and Research Hospital, Türkiye. e-mail: keremkurt43@gmail.com
[2]Department of Pathology, Izmir Katip Celebi University Ataturk Training and Research Hospital, Türkiye. e-mail: drnuket2003@yahoo.com
[3]Department of Ophthalmology, Izmir Katip Celebi University Ataturk Training and Research Hospital, Türkiye. e-mail: seyda.ugurlu@ikcu.edu.tr

ORCID ID: KK: 0000-0003-2526-6908 **NOE:** 0000-0002-7784-5699 **SKU:** 0000-0002-4057-3984

DOI: 10.52818/cjmr.11535853 **E-ISSN:** 2791-7061

ARTICLE INFO

Article Information

Article Type:
Case Report
Received: 26.08.2024
Accepted: 05.02.2025
Published: 30.04.2025

Keywords:
Optic nerve,
Optic nerve glioma,
Pilocytic astrocytoma

ABSTRACT

Optic nerve gliomas are rare tumors that constitute the majority of optic pathway tumors and generally occur in the first two decades. They can be seen anywhere along the optic pathway, with the optic nerve and chiasm being common sites. Most optic nerve gliomas are histologically classified as pilocytic astrocytomas, often associated with neurofibromatosis type 1. While typically presenting with visual impairment, other symptoms, like optic atrophy and proptosis, may also occur. Here, we report two cases of optic nerve glioma in elderly females aged 65 and 79 years, presenting with ocular pain and vision loss. Radiological and histopathological findings showed characteristic features of low-grade glioma. Immunohistochemical staining supported the diagnosis. We found 2 cases worth presenting because of the presence of prolonged symptoms and the advanced age of the patients.

MAKALE BİLGİLERİ

Makale Bilgisi

Makale Türü:
Olgu Sunumu
Geliş Tarihi: 26.08.2024
Kabul Tarihi: 05.02.2025
Yayım Tarihi : 30.04.2025

Anahtar Kelimeler:
Optik sinir,
Optik sinir gliomu,
Pilositik astrositoma

ÖZET

Optik sinir gliomları, optik yolak tümorlerinin çoğunluğunu oluşturan genellikle hayatın ilk 2 yılında görülen nadir tümörlerdir. En sık optik sinirde olmakla beraber optik yolak boyunca yerleşebilir. Çoğu optik sinir gliomaları, genellikle nörofibromatozis tip 1 ile ilişkilendirilen pilositik astrositomalar olarak sınıflandırılmaktadır. Başlıca görme bozukluğu olmakla beraber optik atrofi ve proptoz gibi belirtiler de görülebilir. 65 ve 79 yaşında, sırasıyla göz ağrısı ve görme kaybı ile başvuran 2 kadın hastaya ait iki optik sinir glioma vakasını rapor ediyoruz. Radyolojik ve histopatolojik bulgular, düşük dereceli gliomun karakteristik özelliklerini göstermekle beraber immünohistokimyasal boyama da tanıyı desteklemiştir. Uzun süreli semptomların varlığı ve hastaların ileri yaşta olması sebebiyle 2 vakayı sunmaya değer bulduk.

Kurt K., Ozkavruk Eliyatkin N., Karadeniz Ugurlu S. A Rare Entity: Two Cases of Optic Nerve Glioma in Adults. CJMR 2025; 5(1):37-41
Correspondence to: Kerem Kurt, Department of Pathology, Izmir Katip Celebi University Ataturk Training and Research Hospital, Türkiye.
Authorship Contributions: KK: Writing of the case, literature review, and editing of the manuscript. NOE: Writing of the case, literature review, and determination of the study concept. SKU: Follow-up of the case and data provision
Conflict of Interest: The authors declare no conflict of interests.
Financial Support: None.

Introduction

Optic pathway gliomas are a rare entity primarily occurring in children (1). Optic pathway gliomas can occur anywhere along the optic pathway, including the optic nerve, optic chiasm, optic tracts, optic radiations, or the hypothalamus. Still, the most common location is the optic nerve or chiasm. The vast majority of these are histologically classified as pilocytic astrocytomas (PA), according to the World Health Organization. The most common clinical presentation is visual impairment, while other clinical presentations are optic atrophy and proptosis. These neoplasms may occur sporadically or are associated with neurofibromatosis type 1 (NF1) (2). 10-70% of the cases are associated with NF1 and have a better prognosis (3, 4). Herein, two cases of Optic nerve gliomas (ONG) occurring in adulthood are presented with detailed pathological findings.

Case Report

The authors declare that they received informed consent from the patients to publish this case report.

Two female patients, aged 65 and 79 years old, presented with vision loss and pain for two years and severe pain and discharge in the right eye for one month, respectively. Both patients had corneal tenderness and impaired eye movement. In the orbital ultrasonography of the first patient, there was volume loss in the anterior bulbous oculi and annular enhancement on the anterior medial side. The optic nerve was lateralized and atrophic. In the second patient, intense hyperechogenicity and traction were detected in the vitreous compartment. The first patient had enucleation surgery, while the second underwent eye evisceration.

Macroscopically, the first specimen measured 1.5 cm, with an irregular, brownish-black surface. Sections revealed calcification and fibrosis. The second patient's specimen, a 2.5 cm enucleation sample, contained a 2.2 cm tumoral mass with necrobiotic areas filling the eyeball.

Histopathological findings were similar in both patients. It was generally hypocellular, with enlargement of optic nerve septa and a biphasic growth pattern, which had altering ratios of piloid areas alternating with spongy regions. Cells in these areas have little transparent cytoplasm, and the cytoplasm borders cannot be clearly distinguished. Although minimal atypia and pleomorphism were seen, the nuclei are hyperchromatic. Mitosis wasn't observed. The tumor periphery contained hypervascular areas and consisted of glomeruloid and thick-walled hyalinized vessels. There were also microcystic areas (Figure 1). Histopathological findings favored low-grade glial tumor.

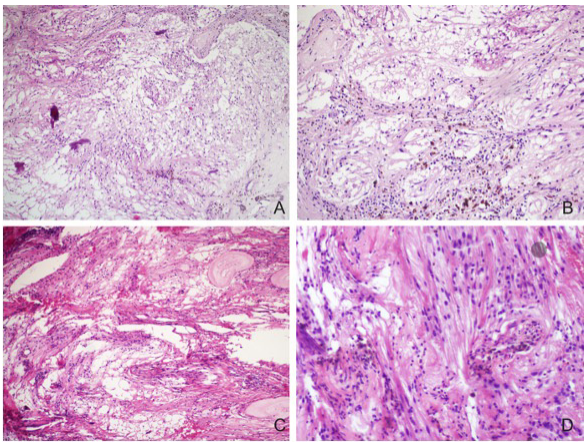

Figure 1. *Histologic features A Biphasic pattern (Hemotoxylene and eosin stain 40X) B Biphasic pattern (Hematoxylin and eosin stain 100X) C Thick-walled hyalinized vessels (Hematoxylin and eosin stain 100X) D cells that have hyperchromatic nucleus and uncertain clear to eosinophilic cytoplasm (Hematoxylin and eosin stain 400X).*

At immunohistochemical analysis, GFAP and S100 protein had positive expression. Expression of IDH and SOX-10 wasn't observed. The Ki-67 proliferation index was 1-2%. There was a positive nuclear expression in ATRX (Figure 2). Melan-A and HMB-45 staining were per-

formed for differential diagnosis of malignant melanoma. Neither marker showed expression. Through these findings, both patients were given a diagnosis of ONG. Genetic analysis wasn't performed because patients didn't have features of NF1, such as cafe-au-lait spots or skin neurofibromas.

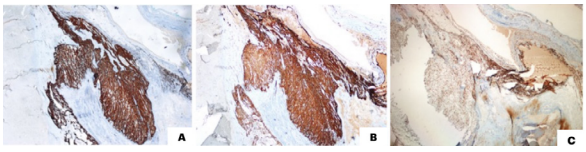

Figure 2. *Immunohistochemical staining A positive expression of GFAP at tumor cells 40x B positive expression of S100 at tumor cells 40x C retained nuclear ATRX immunostaining at tumor cells 40x*

Discussion

ONGs are rare entities that occur early in life and comprise 0.6-3.5% of all orbital tumors (5,6). ONGs are rare in adults and have clinically aggressive patterns (7). Also, they are often histopathologically malign type (8,9). In an extensive series of 445 patients, low-grade tumors were detected in a few patients (10).

Intra-cystic hemorrhage is rare in pediatric ONGs and hasn't been reported in adults. In our two cases, intra-cystic hemorrhage wasn't observed (11).

Patients usually have severe clinical presentations, such as vision loss and proptosis. Our two cases have advanced age and non-acute symptoms. The first patient had pain and progressive vision loss over two years. The second patient had discharge and pain for one month. The slow clinical course may be associated with the histological type being PA.

ONGs are generally WHO grade I PAs with immature astrocytes. Histologically, all PAs show a biphasic pattern with varying proportions of piloid and microcystic areas. Hyalinized vessels are common, especially in patients over thirty. Intracytoplasmic Rosenthal fibers and eosinophilic granular bodies are observed. (12).

In our two cases, they exhibited biphasic patterns with varying proportions of pilocytic and microcystic areas. They contained hypervascular areas composed of hyalinized vessels. Eosinophilic granular bodies and protein droplets weren't observed.

Many cases of PA with a slower course and spontaneous regression have been reported in the literature. Additionally, cases with NF-1 are limited to optic nerve without extra-optic involvement and have a better prognosis.

In differential diagnosis, optic nerve sheath meningiomas share the same localization, but radiological features can help differentiate them from ONGs. Both ONGs and meningiomas can exhibit a diffuse enlargement of the optic nerve, but meningiomas show "tram-tracks," which are caused by the thickened and denser optic nerve sheath, resulting in a central lucency (4).

Immunohistochemical findings are useful in the differentiation of PA from diffuse astrocytomas. PA is diffusely positive for GFAP and Olig-2. Also, vimentin and S-100 protein have positive expression. The complete absence of neurofilament protein staining can be used as proof of a non-infiltrating tumor. Another clue is the expression of IDH-1 in diffuse astrocytomas and its absence in PA. Ki-67 proliferation marker is typically low and <5% (4,12).

Pilomyxoid astrocytoma (PMA) generally occurs in the hypothalamic/chiasmatic area. Histologic appearance is a myxoid background and a monomorphous population of highly piloid astrocytic cells with predominantly angiocentric arrangements. Unlike typical PA, PMAs don't have Rosenthal fibers and a biphasic pattern (4, 12).

The management of ONGs remains controversial (13, 14). Due to rarity, there isn't con-

sensus on standard treatment, especially in adult-type ONGs. Although ONGs grow slowly, continued expansion may be seen in some patients. They can extend into neighboring tissues, including the optic nerve, optic chiasm, and adjacent brain regions. A multidisciplinary approach, crucial for patient management, varies by case. The first choice is observation if patients don't have substantial visual deficits. Surgical resection reduces proptosis and relieves orbital pain in cases of clinical or radiographic progression.

Result

It is crucial to protect the optic nerve during surgical intervention. But, often, there is vision loss. Radiotherapy has continued to be controversial for these tumors. In our cases, it was challenging to determine the boundary between the optic nerve and tumor utilizing imaging and intraoperative results: the optic nerve was entirely superseded by the tumor (15). Hence, preserving the optic nerve was impossible in both cases.

References

1.Burkhard C., Di Patre PL., Schüler D., et al. A population-based study of the incidence and survival rates in patients with pilocytic astrocytoma. J Neurosurg 2003; 98(6):1170-4. Doi: 10.3171/jns.2003.98.6.1170.

2.Binning MJ., Liu JK., Kestle JR., Brockmeyer DL., Walker ML. Optic pathway gliomas: a review. Neurosurg Focus 2007; 23(5):E2. Doi: 10.3171/FOC-07/11/E2.

3.Kuramitsu S., Suzaki N., Takahashi T., et al. Pilocytic astrocytoma of the optic nerve with intracystic hemorrhage in an adult: illustrative case. J Neurosurg Case Lessons 2022; 4(2):CASE22143. Doi: 10.3171/CASE22143.

4.Huang M., Patel J., Patel BC. Optic Nerve Glioma. In: StatPearls [Internet]. Treasure Island, FL: StatPearls Publishing; 2024. Available from: https://www.ncbi.nlm.nih.gov/books/NBK557878/

5.Shields JA., Bakewell B., Augsburger JJ., Flanagan JC. Classification and incidence of space-occupying lesions of the orbit. Arch Ophthalmol 1984; 102(11):1606-11. Doi: 10.1001/archopht.1984.01040031296011.

6.Farazdaghi MK., Katowitz WR., Avery RA. Current treatment of optic nerve gliomas. Curr Opin Ophthalmol 2019; 30(5):356-63. Doi: 10.1097/ICU.0000000000000587.

7.Cummings TJ., Provenzale JM., Hunter SB., et al. Gliomas of the optic nerve: histological, immunohistochemical (MIB-1 and p53), and MRI analysis. Acta Neuropathol 2000; 99(5):563-70. Doi: 10.1007/s004010051161.

8.Campbell AA., Gartrell-Corrado RD., Mansukhani M., et al. SETD2 mutation in an aggressive optic nerve glioma. JAMA Ophthalmol 2020; 138(1):102-4. Doi: 10.1001/jamaophthalmol.2019.4511.

9.Bilgin G., Al-Obailan M., Bonelli L., et al. Aggressive low-grade optic nerve glioma in adults. Neuroophthalmology 2014; 38(6):297-309. Doi: 10.3109/01658107.2014.966851.

10.Mishra MV., Andrews DW., Glass J., et al. Characterization and outcomes of optic nerve gliomas: a population-based analysis. J Neurooncol 2012; 107(3):591-7. Doi: 10.1007/s11060-011-0783-2.

11.van Baarsen K., Roth J., Serova N., et al. Optic pathway-hypothalamic glioma hemorrhage: a series of 9 patients and review of the literature. J Neurosurg 2018; 129(6):1407-15. Doi: 10.3171/2017.8.JNS163085.

12.Grossniklaus HE., Eberhart CG., Kivelä TT. WHO Classification of Tumours of the Eye. 4th ed. Lyon: International Agency for Research on Cancer; 2018.

13.Hill CS., Khan M., Phipps K., et al. Neurosurgical experience of managing optic pathway gliomas. Childs Nerv Syst 2021; 37(6):1917-29. Doi: 10.1007/s00381-021-05060-8.

14.Thomas RP., Gibbs IC., Xu LW., Recht L. Treatment options for optic pathway gliomas. Curr Treat Options Neurol 2015; 17(2):333. Doi: 10.1007/s11940-014-0333-2.

15.Tang Y., Gutmann DH. Neurofibromatosis type 1-associated optic pathway gliomas: current challenges and future prospects. Cancer Manag Res 2023; 15:667-81. Doi: 10.2147/CMAR.S362678.

www.ikcu.edu.tr